

UC Irvine

UC Irvine Previously Published Works

Title

Accelerated microbial turnover but constant growth efficiency with warming in soil

Permalink

<https://escholarship.org/uc/item/2qc5p2vm>

Journal

Nature Climate Change, 4(10)

ISSN

1758-678X

Authors

Hagerty, Shannon B
van Groenigen, Kees Jan
Allison, Steven D
[et al.](#)

Publication Date

2014-10-01

DOI

10.1038/nclimate2361

Peer reviewed

1 **Title page**

2

3 *Title*

4 Accelerated microbial turnover but constant growth efficiency with warming in soil

5

6 *Author affiliations*

7 Shannon B. Hagerty^{*}, Kees Jan van Groenigen^{1,2}, Steven D. Allison³, Bruce A. Hungate^{1,2},
8 Egbert Schwartz¹, George W. Koch^{1,2}, Randall K. Kolka⁴, and Paul Dijkstra^{1,2}

9

10 ¹Department of Biological Sciences, Northern Arizona University, Flagstaff, Arizona

11 86011

12 ² Center for Ecosystem Science and Society, Northern Arizona University, Flagstaff,

13 Arizona 86011

14 ³Department of Ecology and Evolutionary Biology and Department of Earth

15 System Science, University of California, Irvine, California 92697

16 ⁴ USDA Forest Service Northern Research Station, Grand Rapids, Minnesota 55744

17

18

19 * email: sbhagerty@gmail.com

20

21 **Rising temperatures are expected to reduce global soil carbon (C) stocks,**
22 **driving a positive feedback to climate change¹³. However, the mechanisms**
23 **underlying this prediction are not well understood, including how temperature**
24 **affects microbial enzyme kinetics, growth efficiency (MGE), and turnover¹⁵. Here, in**
25 **a laboratory study, we show that microbial turnover accelerates with warming and,**
26 **along with enzyme kinetics, determines the response of microbial respiration to**
27 **temperature change. In contrast, MGE, which is generally thought to decline with**
28 **warming^{6,8}, showed no temperature sensitivity. Using a microbial-enzyme model, we**
29 **show that temperature-sensitive microbial turnover promotes soil C accumulation**
30 **with warming, in contrast to reduced soil C predicted by traditional biogeochemical**
31 **models. Furthermore, the effect of increased microbial turnover differs from the**
32 **effects of reduced MGE, causing larger increases in soil C stocks. Our results**
33 **demonstrate that the response of soil C to warming is affected by changes in**
34 **microbial turnover. This control should be included in the next generation of models**
35 **to improve prediction of soil C feedbacks to warming.**
36
37

38 Many global C cycling models predict reductions in soil C with climate warming³.
39 More recent models that include microbial controls over decomposition suggest a wider
40 range of potential responses⁵. These models reproduce current soil C stocks more
41 accurately than models that do not incorporate microbial dynamics⁹, but their ability to
42 predict soil C responses to climate change is hampered by uncertainty in the temperature
43 sensitivity of microbial processes⁴. There is an active debate in recent literature about
44 which microbial mechanisms should be represented in soil C cycling models^{7,10-13}.

45 Warming increases kinetic energy, accelerating enzyme-requiring reactions¹, and
46 stimulating C consumption by soil microbes. Microbial C consumption and respiration,
47 the largest flux of C out of soil, is significantly affected by both the size and functioning
48 of the soil microbial community^{3,6}. Warming may change the soil microbial biomass
49 carbon (MBC) concentration and activities through two potentially concurrent
50 mechanisms. First, warming can decrease MGE, which is the proportion of substrate C
51 that is used for microbial growth relative to the total amount of substrate C consumed^{7,14}.
52 Higher temperatures are generally expected to reduce MGE, as warming limits microbial
53 growth by increasing the energy cost of maintaining existing biomass⁸. However,
54 responses of MGE in soil microbial communities are equivocal, with studies reporting
55 decreased MGE with temperature increase^{15,16}, no change¹⁴, or a variable response based on
56 substrate type¹⁷. It is unclear to what extent this variability is caused by the methods and
57 procedures used for measuring MGE in soil⁸. Second, warming can affect microbial
58 turnover rates¹⁸. Microbial turnover is determined by microbial cell production and cell
59 death, which are processes that may be affected by temperature. Dead cells may either
60 adhere to soil particles and join the pool of soil organic carbon (SOC) or be metabolized

61 by living microbes¹⁹. Consequently accelerated turnover can increase respiration per unit
62 of MBC even when MGE remains the same²⁰. However, most studies of MGE responses
63 to warming do not account for the respiration and cell death that result from turnover¹⁵⁻¹⁷

64 We determined the temperature sensitivity of MGE and turnover to examine the
65 mechanisms controlling the response of soil C cycling processes to warming. We
66 measured MGE and microbial turnover in mineral soil and organic soil from the Marcell
67 Experimental Forest, Minnesota, after a one week incubation at 5, 10, 15, and 20 °C. We
68 used metabolic tracer probing to determine MGE¹⁴. In this method, MGE is calculated
69 from the fate of individual C-atoms in glucose and pyruvate. Unlike other methods¹⁵⁻¹⁷,
70 metabolic tracer probing method determines an MGE measurement almost entirely
71 unaffected by microbial turnover because it can be done very quickly (1 h or less at room
72 temperature) and calculates MGE based on metabolic modeling. We combined MGE
73 measurements with measurements of microbial respiration and MBC to calculate
74 microbial turnover rates.

75 We found that MGE was not sensitive to temperature (Figure 1). Mean MGE was
76 0.72 (\pm 0.01 SE, n = 22) in mineral soil and 0.71 (\pm 0.01 SE, n = 21) in organic soil.
77 Across all temperature treatments and replicates MGE ranged between 0.67 and 0.75.
78 These values for MGE are high relative to the average values observed in soils and other
79 ecosystems^{7,8,21}. It is also higher than 0.6, an average maximum MGE value for pure
80 culture studies^{8,22} (for further discussion on theoretical thermodynamic constraints of
81 MGE, see Supplementary Note). This high value suggests that the active microbial
82 community functions at a high biochemical efficiency and microorganisms with
83 relatively high maintenance costs contribute little to the total activity. High efficiency

84 values may also indicate additional energy sources (for example from oxalate or
85 formate²³), or direct incorporation of large amounts of cellular compounds, such as amino
86 acids¹⁴. However, what little information is available suggests that these effects will be
87 only slightly affected by temperatures¹⁷.

88 Microbial growth efficiency is generally expected to decline as a result of
89 increased microbial maintenance costs at higher temperatures^{6,7,24}. This effect of
90 temperature on maintenance energy has been observed in a pure culture experiment²⁵, but
91 may not be observable in diverse soil communities where growth optimum temperatures
92 can vary widely between microbial species¹¹. If the composition of the active microbial
93 community shifts, higher maintenance costs might be avoided and MGE could be
94 unchanged. It is also possible that the microbial community expresses physiological
95 acclimation⁶.

96 Despite the constant MGE with temperature, higher temperatures increased
97 microbial respiration in the mineral soil and organic soil by nearly 6-fold and 8-fold,
98 respectively (Supplementary Figure S1). Across the same temperature range, specific
99 respiration rate ($\mu\text{g CO}_2\text{-C mg}^{-1}\text{ MBC h}^{-1}$) increased by 540 % in the mineral soil and 630
100 % in the organic soil. Because increased respiration rates could not be explained by
101 increased microbial biomass, warming must have affected microbial C metabolism by
102 faster C consumption.

103 Higher specific respiration rates and constant MGE with increasing temperature
104 indicate an increased production of new microbial biomass. Warming significantly
105 increased MBC gross production rates ($0.97 \mu\text{g MBC g}^{-1}\text{ dry soil d}^{-1}\text{ }^\circ\text{C}^{-1}$, $r^2 = 0.99$ in
106 mineral soil and $3.63 \mu\text{g MBC g}^{-1}\text{ dry soil d}^{-1}\text{ }^\circ\text{C}^{-1}$, $r^2 = 0.98$ in organic soil). However,

107 temperature did not change the MBC concentration ($p = 0.474$) in either soil
108 (Supplementary Table S1). Therefore, warming increased microbial turnover ($p = 0.02$)
109 in both soils by $0.004 \text{ d}^{-1} \text{ } ^\circ\text{C}^{-1}$ in mineral soil and by $0.003 \text{ d}^{-1} \text{ } ^\circ\text{C}^{-1}$ in organic soil (Figure 2),
110 compensating for increased MBC production.

111 Why did warming increase microbial turnover? One possibility is that the
112 abundance or activity of microbial predators and grazers increased with temperature.
113 However, the few studies examining the effect of warming on microbial predator and
114 grazer abundances have found both increases and decreases in abundances after several
115 years of warming³⁶. Warming could cause a shift in the microbial community composition
116 that drives faster turnover. Natural senescence of microbial cells may also be accelerated
117 as protein turnover is increased at higher temperatures¹⁸. Alternatively, at higher
118 temperatures and greater MBC productivity, activity of viruses could increase cell death.
119 Each of these mechanisms may respond differently to temperature and could be important
120 to informing our understanding of responses of soil C fluxes to temperature increases.

121 An increase in turnover with warming may partly explain the generally observed
122 decline in MGE with temperature. Previous studies that suggest a decline in MGE did not
123 separate the influences of turnover and MGE on the residence time of carbon tracers in
124 the soil microbial biomass. Ideally, MGE is determined during a very short period after
125 addition of ^{13}C -labeled C compounds (instantaneous MGE or MGE_i). But over time,
126 microbial turnover will cause some of the ^{13}C initially incorporated into microbial biomass
127 to be released as CO_2 , resulting in an overestimation of CO_2 production and an
128 underestimation of microbial biomass production and $\text{MGE}^{16,21}$. This effect increases with

129 incubation duration and may cause differences in apparent MGE (MGE_A), especially
130 when microbial turnover rates differ between treatments (as in this study, Figure 2).

131 We modeled the effects of assay duration and temperature on MGE_A (Figure 3a).
132 Assuming an MGE_i of 0.72 for all temperatures and microbial turnover rates as
133 determined in this study (Figure 2), we estimate that MGE_A declines by $0.005\text{ }^\circ\text{C}^{-1}$ in
134 mineral (Figure 3b) and $0.003\text{ }^\circ\text{C}^{-1}$ in organic soil after a two-day incubation. Other
135 studies have found that MGE declines by $0.009\text{ }^\circ\text{C}^{-1}$ (ref. 15) to $0.017\text{ }^\circ\text{C}^{-1}$ (ref. 1) when
136 measuring MGE over 24-48 h. These rates of decline with temperature are greater than
137 those in this study, however it remains unclear whether this is associated with higher
138 turnover rates in those studies or with genuine declines in MGE_i . Studies that have used
139 short-term assays (<6 h) reported no change in MGE of soil microbial communities with
140 warming^{14,17}, consistent with results we report here (Figure 1).

141 We found that microbial turnover rate is temperature sensitive, but that MGE is
142 not. These results were determined in a short-term laboratory incubation, a controlled
143 environment which provides the best conditions to test mechanistic questions like those
144 in this study. On a longer time scale, turnover rates and MGE could be indirectly
145 affected by temperature through nutrient limitation, changes in community composition,
146 and changes in soil moisture. It is also likely that across a large spatial scale turnover
147 rates will vary; we saw differences in turnover rate between the two soils studied here
148 (Figure 2). Other studies have found that warming decreases MBC, indicating
149 accelerated microbial turnover could be important at time scales longer than in this
150 study^{27,28}. However, accelerated microbial turnover in response to warming is a mechanism
151 that has never been explicitly accounted for in soil carbon models.

152 In order to assess the implications of microbial turnover to soil C predictions, we
153 used the Allison-Wallenstein-Bradford (AWB) model⁵⁶. The AWB model uses rates of
154 microbial processes that are based on the best estimate of steady state conditions, which
155 allowed us to extrapolate the significance of our short-term results to long-term steady-
156 state C stocks. We simulated three different scenarios. In the first scenario, neither MGE
157 nor turnover was altered by temperature and soil C decomposition was modeled with a
158 first-order decay function and Michaelis-Menten enzyme kinetics, the current assumption
159 in most biogeochemical models^{7,29}. In this scenario there was no change in MBC with
160 warming and SOC declined as a result of accelerated enzymatic decomposition (Figure
161 4). In the second scenario, MGE decreased by $0.016\text{ }^{\circ}\text{C}^{-1}$, as in prior theoretical studies⁶.
162 Here, the reduction in MGE limited microbial growth at higher temperatures, resulting in
163 a 5 % decline of $\text{MBC }^{\circ}\text{C}^{-1}$ averaged from 5 to 20 °C. As a result, SOC increased with
164 temperature as decomposition became limited by MBC. The third scenario corresponded
165 to our experimental observations of a constant MGE and accelerated microbial turnover
166 with warming. Accelerated microbial turnover at higher temperature caused decreases in
167 MBC and increase in SOC, which were larger than for the scenario of constant turnover
168 and declines in MGE. We conclude that, although MGE did not decline, accelerated
169 microbial turnover is an alternative mechanism that can moderate the effects of
170 temperature on soil C stocks. These model simulations suggest that temperature-sensitive
171 microbial turnover produces an effect on MBC and SOC that is not accounted for in
172 current biogeochemical or microbial models.

173 Our results show that accelerated enzyme kinetics and increased microbial
174 turnover are the main mechanisms associated with an increased respiration at higher

175 temperatures and, in model simulations, lead to a small increase in SOC content under
176 elevated temperatures. This effect on SOC is similar to those that have been predicted in
177 models assuming a decline in MGE, but differs in direction from the predictions
178 traditional biogeochemical models. Consequently, soil microbial models should include a
179 temperature-sensitive microbial turnover rate. The lack of temperature sensitivity in
180 MGE, which is controlled at the cellular level, suggests that microbial biochemical
181 efficiency is a weak control on soil C dynamics.

182

183 **Methods**

184 Soil samples were collected in October 2012 from the Marcell Experimental
185 Forest in Grand Rapids, MN (MAT = 3°C, MAP = 750 mm). Mineral soil samples were
186 collected from the A horizon in a hardwood forest and organic soil samples were
187 collected from an ombrotrophic peatland (top 40 cm after removing the living layer of
188 moss). Soil samples were stored at 4 °C until the experiment began in April 2013.

189 Replicates (n = 6) from both soils were randomly assigned to one of four incubators and
190 incubated for seven days at 5, 10, 15, or 20 °C (See Supplementary Methods Section I).

191 After a seven-day incubation period, MGE was determined using two position-
192 specific ¹³C-labeled isotopologues of glucose (U-¹³C and 1-¹³C) and two of pyruvate (1-¹³C
193 and 2,3-¹³C) as metabolic tracers^{14,30}. We measured ¹³CO₂ accumulation in each jar three
194 times over the course of 60, 90, 135, or 180 min at 20, 15, 10, and 5 °C respectively. The
195 ratios between ¹³CO₂ production rates from glucose and pyruvate isotopologues were
196 calculated and used to model metabolic pathway activities and MGE¹⁰ (Table S2). One
197 complete replicate (i.e. 4 temperatures x 2 soils x 4 isotopologues) was incubated and

198 analyzed each week. For more details and background information on metabolic probing
199 and modeling, see Supplementary Methods Section II and Figure S2.

200 Two weeks after the MGE measurements, another incubation was set up under
201 identical conditions to measure respiration and MBC. Each of the four incubators was
202 systematically assigned to one of the four treatment temperatures and both soils were
203 incubated for seven days. After the seven-day incubation period, CO₂ concentrations
204 were measured at 0 and 24 h. After the respiration measurement, MBC concentration was
205 measured using chloroform fumigation-extraction (See Supplementary Methods Section
206 III, Table S1).

207 We calculated microbial turnover using the experimentally measured respiration
208 (*R*), MGE, and MBC (Supplementary Methods Section IV, Figure S3). We applied the
209 assumptions that MBC was at steady state and that all turned over MBC was released as
210 CO₂. Our findings of temperature-sensitive turnover were not affected much by non-
211 steady state of MBC and whether C from turnover was released as CO₂ or added to the
212 SOC pool (Supplementary Methods Section V, Figure S4 and S5).

213 The gross microbial production was calculated as

$$214 \quad \Delta MBC_g = MGE * R,$$

215 and microbial turnover (τ) assuming steady state MBC pools and all C from turnover
216 going to CO₂ as follows

$$217 \quad \tau = \frac{MGE * R}{MBC}$$

218

219 To calculate the effect of microbial turnover and incubation duration on MGE_A, we used
220 the following equation

221 $MGE_n = (1 - \tau)^n \times MGE_i$

222 with n in days. In this calculation, MGE_i was set at 0.72 for all temperature treatments,
223 while turnover rates were those measured for mineral soil in this experiment (Figure 2).
224 See supplementary methods section VI for more information.

225 We analyzed all experimental data using a multifactor ANOVA with temperature
226 and soil type as the main factors. To calculate turnover from experimental data, we used
227 bootstrap resampling to calculate 95 % confidence intervals. Additional details on all
228 statistical analyses can be found in Supplementary Methods Section VII.

229 We modeled the consequences of accelerated microbial turnover with warming,
230 declining MGE with warming, and constant microbial turnover and MGE using the
231 Allison-Wallenstein-Bradford microbial model (Supplementary Methods Section VIII,
232 Table S3).

233

234

235

236 Literature Cited

- 237 1. Davidson, E. A. & Janssens, I. A. Temperature sensitivity of soil carbon
238 decomposition and feedbacks to climate change. *Nature* **440**, 165-173,
239 doi:10.1038/nature04514 (2006).
- 240 2. Cox, P. M., Betts, R. A., Jones, C. D., Spall, S. A. & Totterdell, I. J. Acceleration of
241 global warming due to carbon-cycle feedbacks in a coupled climate model.
242 *Nature* **408**, 184-187, doi:10.1038/35041539 (2000).
- 243 3. Schlesinger, W. H. & Andrews, J. A. Soil respiration and the global carbon cycle.
244 *Biogeochemistry* **48**, 7-20, doi:10.1023/a:1006247623877 (2000).
- 245 4. Ågren, G. I. & Wetterstedt, J. A. M. What determines the temperature response of
246 soil organic matter decomposition? *Soil Biology & Biochemistry* **39**, 1794-
247 1798, doi:10.1016/j.soilbio.2007.02.007 (2007).
- 248 5. Li, J. W., Wang, G. S., Allison, S. D., Mayes, M. A. & Luo, Y. Q. Soil carbon sensitivity
249 to temperature and carbon use efficiency compared across microbial-
250 ecosystem models of varying complexity. *Biogeochemistry* **119**, 67-84,
251 doi:10.1007/s10533-013-9948-8 (2014).
- 252 6. Allison, S. D., Wallenstein, M. D. & Bradford, M. A. Soil-carbon response to
253 warming dependent on microbial physiology. *Nature Geoscience* **3**, 336-340,
254 doi:10.1038/ngeo846 (2010).
- 255 7. Manzoni, S., Taylor, P., Richter, A., Porporato, A. & Ågren, G. I. Environmental and
256 stoichiometric controls on microbial carbon-use efficiency in soils. *New*
257 *Phytologist* **196**, 79-91, doi:10.1111/j.1469-8137.2012.04225.x (2012).

- 258 8. Sinsabaugh, R. L., Manzoni, S., Moorhead, D. L. & Richter, A. Carbon use efficiency
259 of microbial communities: stoichiometry, methodology and modelling.
260 *Ecology Letters* **16**, 930-939, doi:10.1111/ele.12113 (2013).
- 261 9. Wieder, W. R., Bonan, G. B. & Allison, S. D. Global soil carbon projections are
262 improved by modelling microbial processes. *Nature Climate Change* **3**, 909-
263 912, doi:10.1038/nclimate1951 (2013).
- 264 10. Schimel, J. P. & Schaeffer, S. M. Microbial control over carbon cycling in soil.
265 *Frontiers in Microbiology* **3**, doi:10.3389/fmicb.2012.00348 (2012).
- 266 11. Billings, S. A. & Ballantyne, F. How interactions between microbial resource
267 demands, soil organic matter stoichiometry, and substrate reactivity
268 determine the direction and magnitude of soil respiratory responses to
269 warming. *Global Change Biology* **19**, 90-102, doi:10.1111/gcb.12029 (2013).
- 270 12. Allison, S. D. A trait-based approach for modelling microbial litter
271 decomposition. *Ecology Letters* **15**, 1058-1070, doi:10.1111/j.1461-
272 0248.2012.01807.x (2012).
- 273 13. Manzoni, S., Schaeffer, S. M., Katul, G., Porporato, A. & Schimel, J. P. A theoretical
274 analysis of microbial eco-physiological and diffusion limitations to carbon
275 cycling in drying soils. *Soil Biology & Biochemistry* **73**, 69-83,
276 doi:10.1016/j.soilbio.2014.02.008 (2014).
- 277 14. Dijkstra, P. *et al.* Effect of temperature on metabolic activity of intact microbial
278 communities: Evidence for altered metabolic pathway activity but not for
279 increased maintenance respiration and reduced carbon use efficiency. *Soil*

- 280 *Biology & Biochemistry* **43**, 2023-2031, doi:10.1016/j.soilbio.2011.05.018
281 (2011).
- 282 15. Steinweg, J. M., Plante, A. F., Conant, R. T., Paul, E. A. & Tanaka, D. L. Patterns of
283 substrate utilization during long-term incubations at different temperatures.
284 *Soil Biology & Biochemistry* **40**, 2722-2728,
285 doi:10.1016/j.soilbio.2008.07.002 (2008).
- 286 16. Tucker, C. L., Bell, J., Pendall, E. & Ogle, K. Does declining carbon-use efficiency
287 explain thermal acclimation of soil respiration with warming? *Global Change*
288 *Biology* **19**, 252-263, doi:10.1111/gcb.12036 (2013).
- 289 17. Frey, S. D., Lee, J., Melillo, J. M. & Six, J. The temperature response of soil
290 microbial efficiency and its feedback to climate. *Nature Climate Change* **3**,
291 395-398, doi:10.1038/nclimate1796 (2013).
- 292 18. Joergensen, R. G., Brookes, P. C. & Jenkinson, D. S. Survival of the soil microbial
293 biomass at elevated-temperatures. *Soil Biology & Biochemistry* **22**, 1129-
294 1136, doi:10.1016/0038-0717(90)90039-3 (1990).
- 295 19. McGill, W. B., Shields, J. A. & Paul, E. A. Relation between carbon and nitrogen
296 turnover in soil organic fractions of microbial origin. *Soil Biology &*
297 *Biochemistry* **7**, 57-63, doi:10.1016/0038-0717(75)90032-2 (1975).
- 298 20. Kaiser, C., Franklin, O., Dieckmann, U. & Richter, A. Microbial community
299 dynamics alleviate stoichiometric constraints during litter decay. *Ecology*
300 *Letters* **17**, 680-690, doi:10.1111/ele.12269 (2014).
- 301 21. Frey, S. D., Gupta, V., Elliott, E. T. & Paustian, K. Protozoan grazing affects
302 estimates of carbon utilization efficiency of the soil microbial community. *Soil*

- 303 *Biology & Biochemistry* **33**, 1759-1768, doi:10.1016/s0038-0717(01)00101-
304 8 (2001).
- 305 22. Roels, J. A. Application of macroscopic principles to microbial-metabolism.
306 *Biotechnology and Bioengineering* **22**, 2457-2514,
307 doi:10.1002/bit.260221202 (1980).
- 308 23. Gommers, P. J. F., Vanschie, B. J., Vandijken, J. P. & Kuenen, J. G. Biochemical limits
309 to microbial-growth yields - an analysis of mixed substrate utilization.
310 *Biotechnology and Bioengineering* **32**, 86-94, doi:10.1002/bit.260320112
311 (1988).
- 312 24. van Bodegom, P. Microbial maintenance: A critical review on its quantification.
313 *Microbial Ecology* **53**, 513-523, doi:10.1007/s00248-006-9049-5 (2007).
- 314 25. Crowther, T. W. & Bradford, M. A. Thermal acclimation in widespread
315 heterotrophic soil microbes. *Ecology Letters* **16**, 469-477,
316 doi:10.1111/ele.12069 (2013).
- 317 26. Blankinship, J. C., Niklaus, P. A. & Hungate, B. A. A meta-analysis of responses of
318 soil biota to global change. *Oecologia* **165**, 553-565, doi:10.1007/s00442-
319 011-1909-0 (2011).
- 320 27. Frey, S. D., Drijber, R., Smith, H. & Melillo, J. Microbial biomass, functional
321 capacity, and community structure after 12 years of soil warming. *Soil*
322 *Biology & Biochemistry* **40**, 2904-2907, doi:10.1016/j.soilbio.2008.07.020
323 (2008).

- 324 28. Curtin, D., Beare, M. H. & Hernandez-Ramirez, G. Temperature and Moisture
325 Effects on Microbial Biomass and Soil Organic Matter Mineralization. *Soil Sci.*
326 *Soc. Am. J.* **76**, 2055-2067, doi:10.2136/sssaj2012.0011 (2012).
- 327 29. Manzoni, S. & Porporato, A. Soil carbon and nitrogen mineralization: Theory and
328 models across scales. *Soil Biology & Biochemistry* **41**, 1355-1379,
329 doi:10.1016/j.soilbio.2009.02.031 (2009).
- 330 30. Dijkstra, P. *et al.* Probing carbon flux patterns through soil microbial metabolic
331 networks using parallel position-specific tracer labeling. *Soil Biology &*
332 *Biochemistry* **43**, 126-132, doi:10.1016/j.soilbio.2010.09.022 (2011).

333

334

335

336 **Acknowledgements**

337 E. Miller contributed to experimental work and N. Aspelin assisted with soil sample
338 collection. This research is supported by an NSF grant (DEB-1146449) to Paul Dijkstra
339 and NSF MRI (DBI-0723250 and 1126840) to George Koch and Tom Whitham.

340

341 **Author contributions**

342 SBH, PD, ES, BAH, and GWK conceived the project, SBH conducted the soil incubation
343 experiment and led the manuscript preparation. RK guided site selection and provided the
344 soils in the study. SBH, KJvG, and PD contributed to data analysis and interpretation,
345 and SDA did the microbial-enzyme modeling. All authors contributed to writing the final
346 manuscript.

347

348 **Additional information**

349 Supplementary information is available in the online version of the paper. Reprints
350 and permissions information is available online at www.nature.com/reprints.

351 Correspondence and requests for materials should be addressed to SBH.

352

353 **Competing financial interests**

354 The authors declare no competing financial interests

355

356

357 **Figure legends**

358 **Figure 1. Microbial Growth Efficiency (MGE) after a 7-day incubation at different**

359 **temperatures for a mineral and an organic soil.** Means and se (n = 6, except for

360 mineral soil at 5, 10 °C and organic soil at 5 °C, where n = 5). There was no significant

361 effect of soil type (p = 0.21) or temperature (p = 0.70) on MGE.

362

363 **Figure 2. Turnover rates (τ , d⁻¹) as a function of temperature for a mineral and an**

364 **organic soil.** The experimental values were resampled using bootstrap method in order to

365 calculate a 95 % confidence interval (error bars). For each soil type, the turnover rate at

366 5 °C is significantly different from that at 20 °C.

367

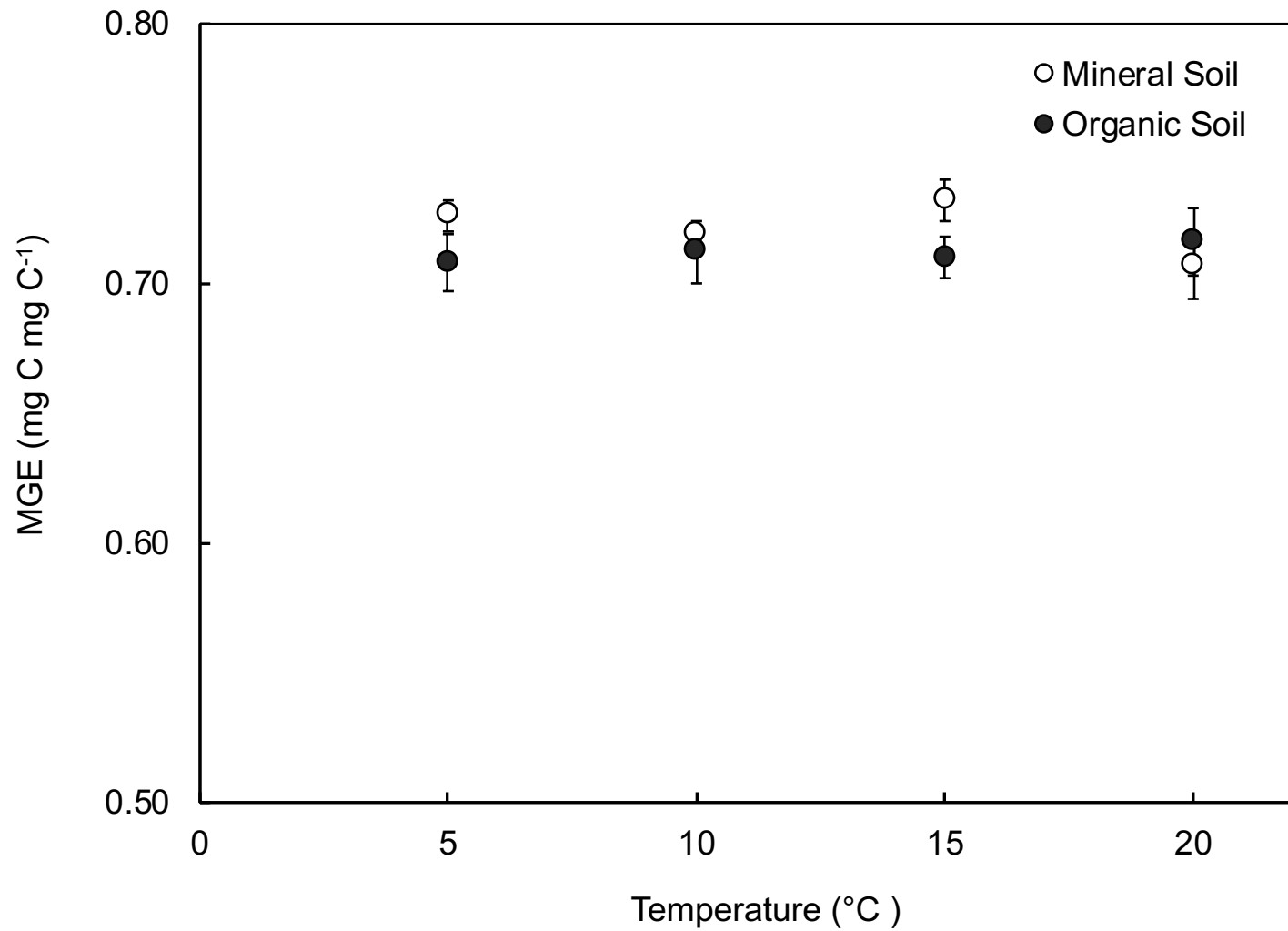
368 **Figure 3. Modeled effect of temperature and incubation duration on apparent**

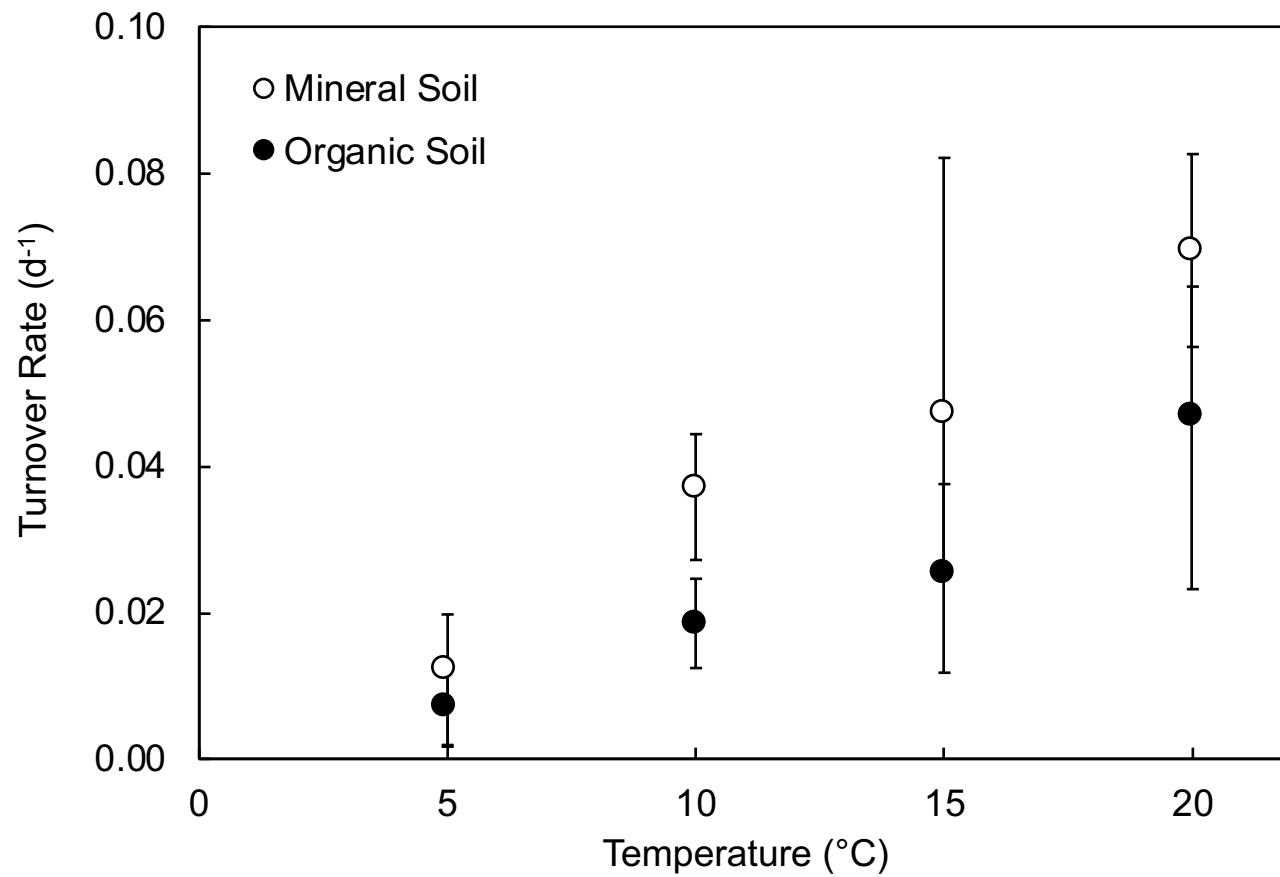
369 **MGE.** a) The relationship between temperature and MGE_a over time was modeled using

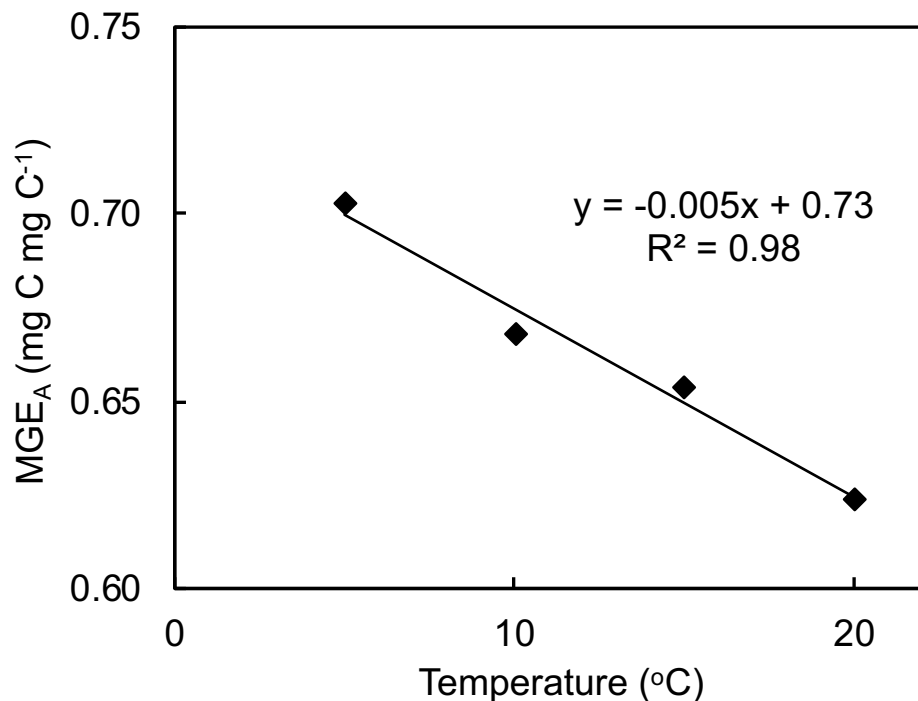
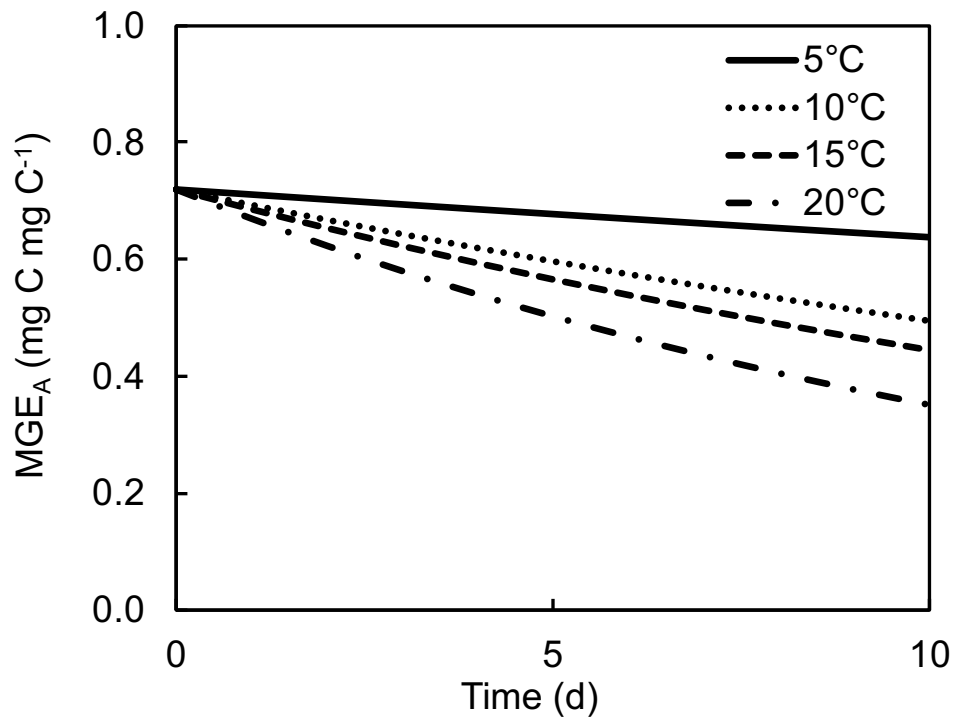
370 the microbial turnover rates for the mineral soil in our study (Figure 2). b) The modeled
371 relationship of MGE_A and temperature in mineral soil after two days.

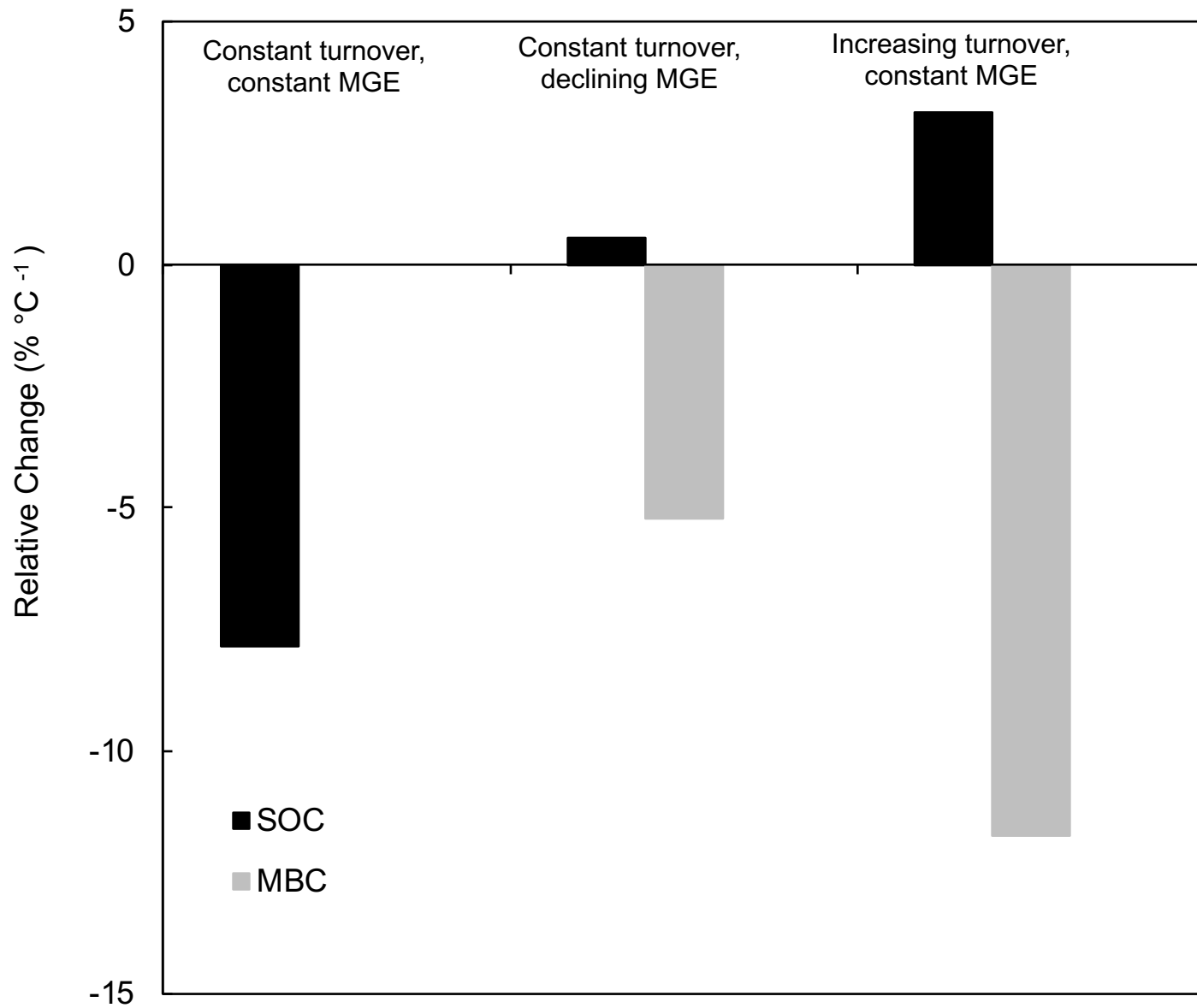
372

373 **Figure 4. The relative change in soil organic C (SOC) and microbial biomass C**
374 **(MBC) from 5 to 20 °C under three scenarios using the Allison-Wallenstein-**
375 **Bradford model.** In the constant turnover, constant MGE scenario there is no change in
376 MBC with temperature.





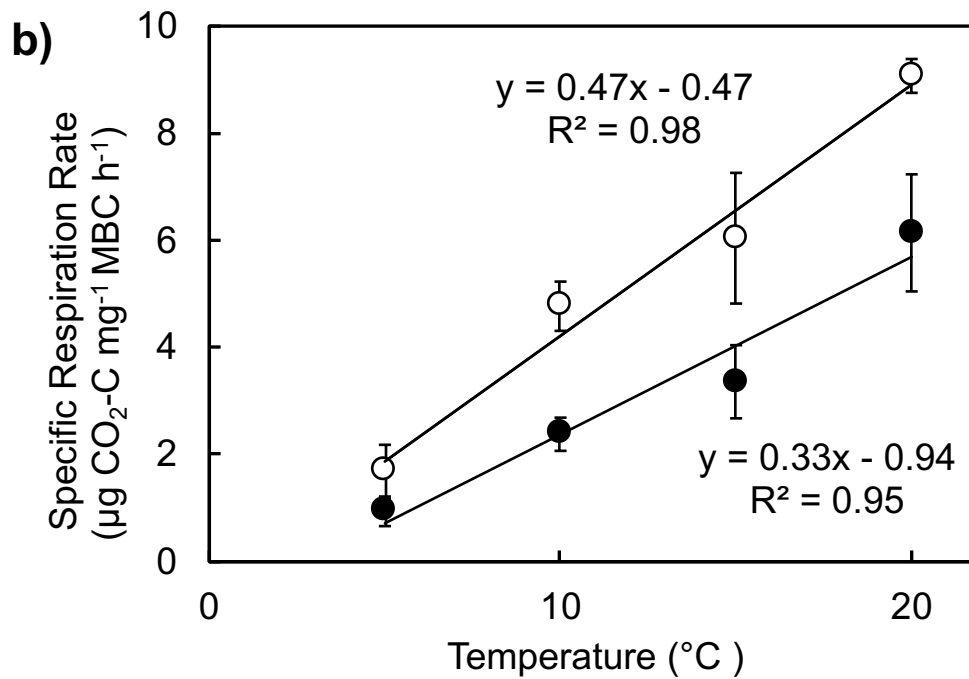
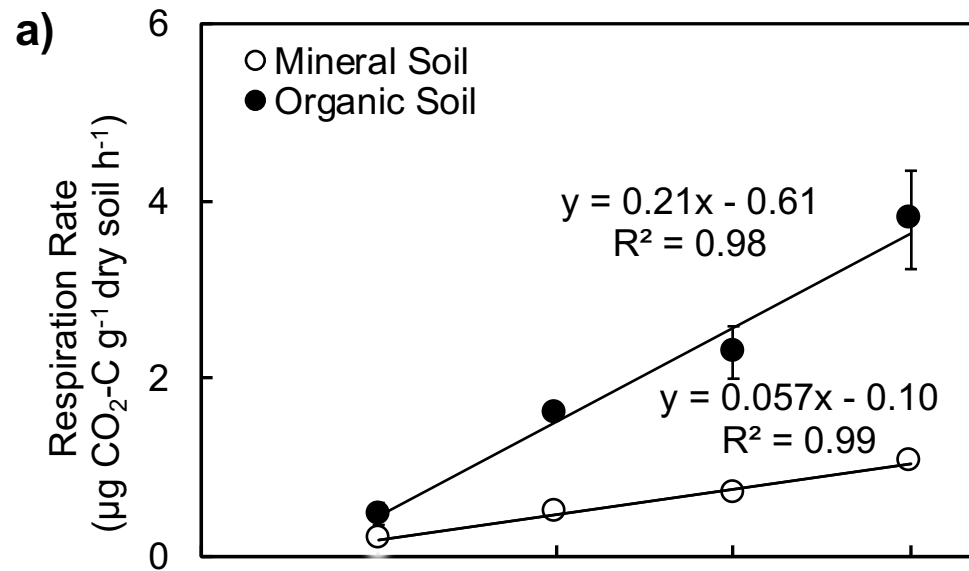


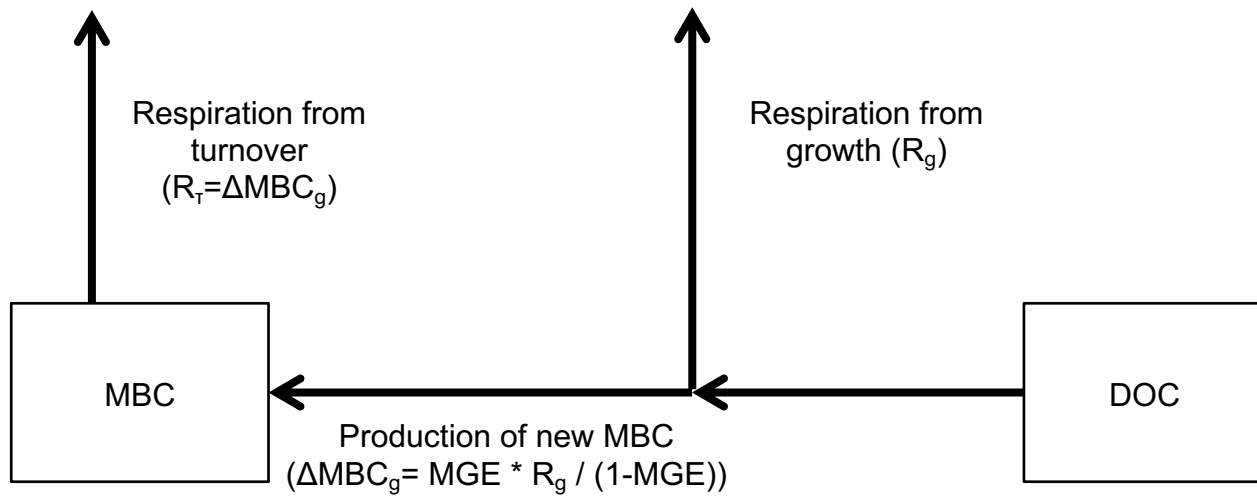


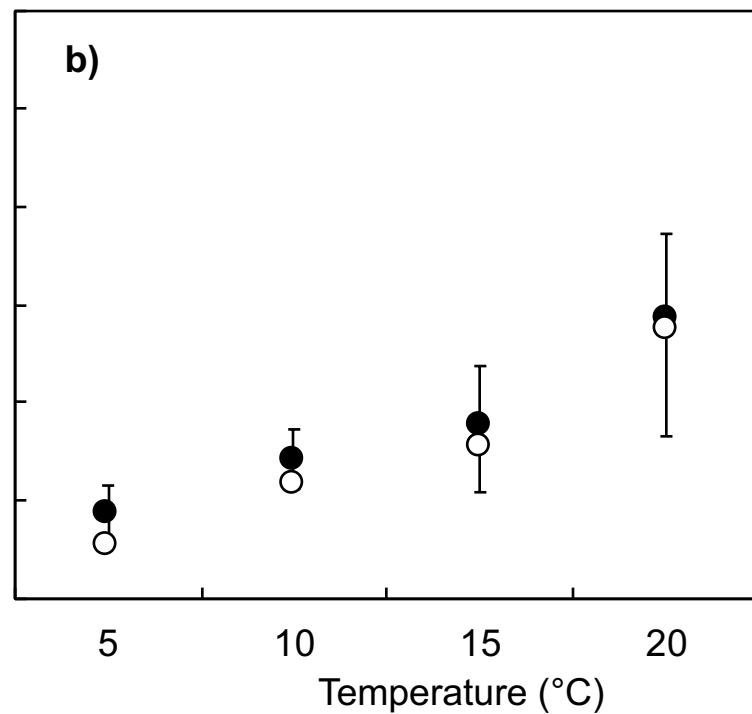
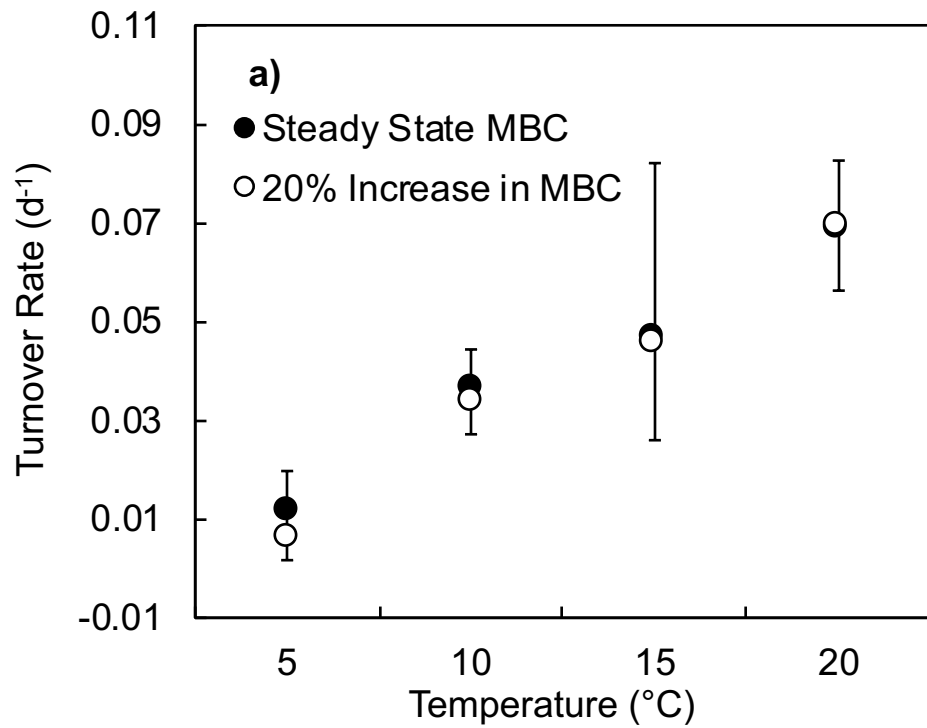
Temperature (°C)	MBC ($\mu\text{g g}^{-1}$ dry soil)		MBN ($\mu\text{g g}^{-1}$ dry soil)	
	Mineral Soil	Organic Soil	Mineral Soil	Organic Soil
5	276 \pm 33	1,229 \pm 117	37.7 \pm 2.4	120 \pm 9.4
10	236 \pm 8.8	1,585 \pm 200	35.8 \pm 0.7	165 \pm 32
15	282 \pm 43	1,623 \pm 170	36.9 \pm 3.2	182 \pm 16
20	263 \pm 9.3	1,412 \pm 81	35.0 \pm 3.0	139 \pm 7.7

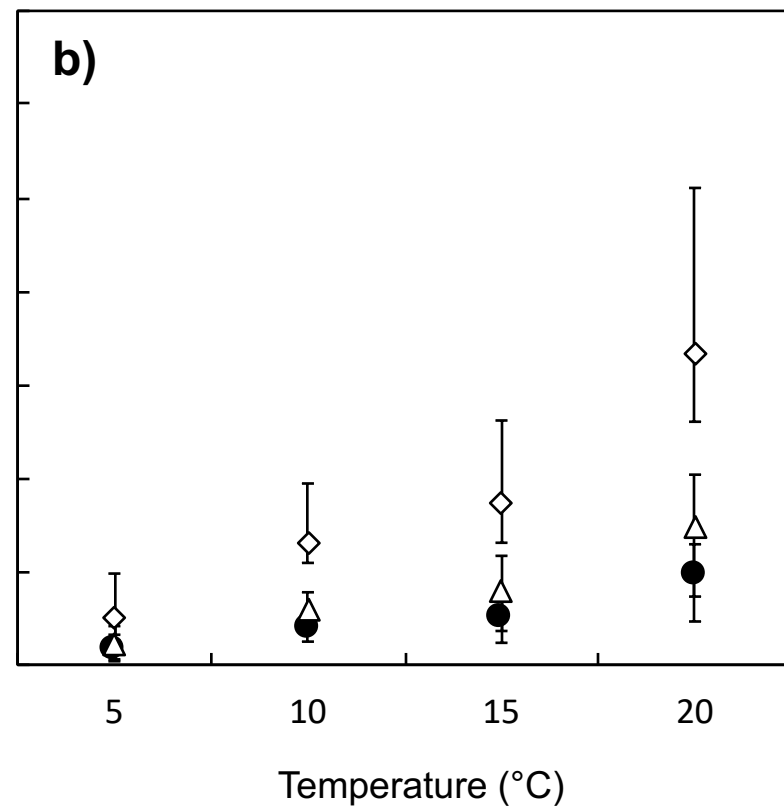
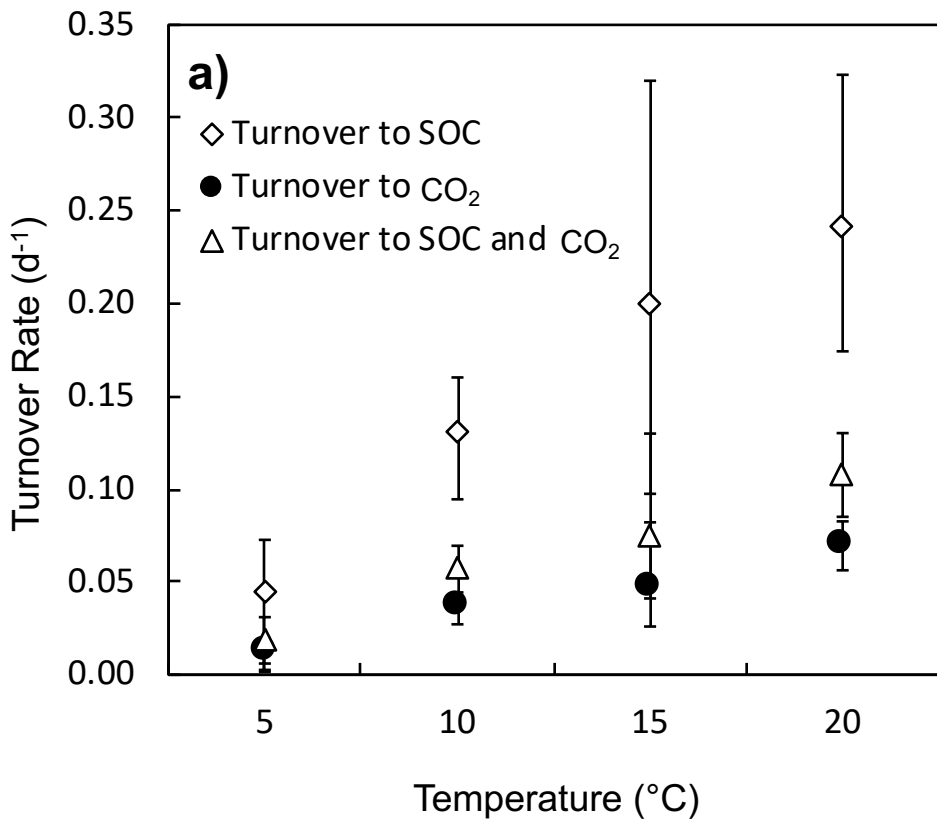
Temperature (°C)	C _U /C ₁ Ratio of Glucose		C ₁ /C ₂₃ Ratio of Pyruvate	
	Mineral Soil	Organic Soil	Mineral Soil	Organic Soil
5	3.21 ± 0.31	2.92 ± 0.24	4.41 ± 0.40	3.56 ± 0.20
10	3.26 ± 0.15	2.91 ± 0.14	3.38 ± 0.20	3.73 ± 0.35
15	3.60 ± 0.39	2.94 ± 0.16	3.75 ± 0.30	3.51 ± 0.19
20	2.70 ± 0.12	3.15 ± 0.26	3.94 ± 0.46	3.61 ± 0.31

Parameter	Description	Value	Units
T_{ref}	Reference temperature	20	°C
MGE_{ref}	MGE at reference temperature	0.31	
m	MGE change with temperature	[0, -0.016]	°C ⁻¹
I_S	SOC input rate	0.00015	mg C g ⁻¹ soil h ⁻¹
I_D	DOC input rate	0.00001	mg C g ⁻¹ soil h ⁻¹
V_{ref}	SOC reference V_{max}	1	mg C mg ⁻¹ C h ⁻¹
$V_{U,ref}$	DOC uptake reference V_{max}	0.01	mg C mg ⁻¹ MBC h ⁻¹
K_{ref}	SOC reference K_m	250	mg C g ⁻¹ soil
$K_{U,ref}$	DOC uptake reference K_m	0.26	mg C g ⁻¹ soil
$r_{B,ref}$	Reference MBC turnover rate	0.00028	mg C mg ⁻¹ C h ⁻¹
Ea_V	SOC V_{max} activation energy	47	kJ mol ⁻¹ K ⁻¹
Ea_{VU}	Uptake V_{max} activation energy	47	kJ mol ⁻¹ K ⁻¹
Ea_K	SOC K_m activation energy	30	kJ mol ⁻¹ K ⁻¹
Ea_{KU}	Uptake K_m activation energy	30	kJ mol ⁻¹ K ⁻¹
Ea_r	MBC turnover activation energy	47	kJ mol ⁻¹ K ⁻¹
r_E	Enzyme production rate	5.6×10^{-6}	mg C mg ⁻¹ MBC h ⁻¹









1 **Accelerated microbial turnover but constant growth efficiency with warming in soil**

2 Shannon B. Hagerty, Kees Jan van Groenigen, Steven D. Allison, Bruce A. Hungate,

3 Egbert Schwartz, George W. Koch, Randall K. Kolka, and Paul Dijkstra

4

5

6 **SUPPLEMENTARY METHODS**

7 ***I. Sample Collection and Incubation***

8 In October 2012, mineral and organic soil was collected from the Marcell
9 Experimental Forest near Grand Rapids, Minnesota on the same day. Organic soil
10 samples were taken from the top 40 cm of an ombrotrophic peatland (i.e. bog), dominated
11 by black spruce (*Picea mariana*) and covered with sphagnum moss (*Sphagnum* sp.). The
12 peat was a Greenwood peat (C content 54.5 %, N content 1.58 %). The mineral soil was a
13 Warba Fine Sandy Loam (C content 6.5 %, N content 0.34 %), collected from the A
14 horizon of a mixed hardwood forest dominated by aspen (*Populus* sp.), maple (*Acer* sp.),
15 and basswood (*Tilia americana*). Mean annual temperature at the site is 3 °C and mean
16 annual precipitation is 750 mm. Soil was shipped overnight on ice to Northern Arizona
17 University where the mineral soil was sieved (4 mm mesh). The organic soil was air-
18 dried to 400 % soil moisture content and live roots were removed by hand. Soil was
19 stored at 4 °C until the start of the experiment.

20 In April 2013, we incubated soil at four temperatures (5, 10, 15, and 20 °C) for
21 seven days before metabolic tracer addition in Precision™ Refrigerated Incubators
22 (Thermo Fisher Scientific Inc, Waltham, MA, USA). Each of the four incubators was
23 randomly assigned to one of four temperatures each week for six weeks, resulting in six

24 replicates of all soil x temperature x isotopologue combinations. For the organic soil
25 incubated at 5 °C, one replicate was lost. Each replicate consisted of four jars, as is
26 required for the metabolic tracer probing¹. Mineral soil (25 g dry weight, 66.5 % soil
27 moisture content) and organic soil (4 g dry weight, 400 % soil moisture content) was
28 incubated in specimen cups and placed in mason jars (473 mL). Mason jars were initially
29 covered with Saran™ plastic wrap, to limit moisture loss but allow oxygen into the jars
30 during the seven-day incubation period. We used iButton data loggers (Maxim Integrated,
31 San Jose, CA, USA) to monitor soil temperature during the incubation and the metabolic
32 tracer probing experiment.

33

34 *II. Position-Specific ¹³C-Labeled Metabolic Tracer Experiment*

35 After incubating the soil for one week, headspace was refreshed before the jar was
36 closed using an airtight lid with a septum. Next, 10 ml of pure CO₂ was added to each jar
37 in order to meet the CO₂ concentration and amount required by the Picarro G2201-*i* CO₂
38 cavity ring-down isotope spectrometer (Picarro Inc., Sunnyvale, CA, USA). Thirty
39 minutes after addition of CO₂, we took a sample of the headspace (time=0). We then
40 added one of four metabolic tracer isotopomers to each of the four parallel incubations
41 per replicate, following the procedure in Dijkstra et al.¹². We used two glucose
42 isotopologues (U-¹³C and 1-¹³C) and two pyruvate isotopologues (1-¹³C and 2,3-¹³C). All of
43 the metabolic tracers were dissolved in deionized water at a concentration of 10.7 μmol C
44 per mL. Two mL of tracer was added to each incubation, equivalent to 10.3 μg C g⁻¹ dry
45 mineral soil and 64.3 μg C g⁻¹ dry organic soil. After tracer addition, 10 ml of headspace

46 was sampled three times at 20 min intervals in the 20 °C incubation, at 30 min intervals
47 at 15 °C, at 45 min intervals at 10 °C, and at 60 min intervals at 5 °C.

48 All gas samples were analyzed on the Picarro G2201-*i* CO₂ cavity ringdown
49 isotope spectrometer. The ratios of ¹³C production for each isotopologue pair were
50 calculated as:

$$51 \quad \frac{C_U}{C_1} \text{ ratio} = \frac{{}^{13}\text{CO}_2 \text{ production from U-}^{13}\text{C glucose}}{{}^{13}\text{CO}_2 \text{ production from 1-}^{13}\text{C glucose}} \quad (1)$$

52 and

$$53 \quad \frac{C_1}{C_{2,3}} \text{ ratio} = \frac{{}^{13}\text{CO}_2 \text{ production from 1-}^{13}\text{C pyruvate}}{{}^{13}\text{CO}_2 \text{ production from 2,3-}^{13}\text{C pyruvate}} \quad (2)$$

54 The C_U/C₁ ratio for glucose and the C₁/C_{2,3} ratio for pyruvate are determined by the
55 characteristics of the central C metabolic network (i.e. glycolysis, citric acid cycle, and
56 pentose phosphate pathway, Figure S2) which cause some C-atoms to be preferentially
57 used for biosynthesis (for example in lipids and amino acids), while others are
58 preferentially lost in decarboxylation reactions. If cells use substrate mainly for the
59 production of ATP and very little for biosynthesis (substrate-limited microbial activity),
60 the C_U/C₁ ratio for glucose will be close to 6:1 (all C-atoms are being released as CO₂),
61 and the C₁/C_{2,3} ratio of pyruvate be close to 1:2. Observed ratios (Table S2) for glucose
62 and pyruvate were significantly different from the expected values for microbes without
63 biosynthesis (p < 0.05).

64 The calculated ratios (Table S2) were used to model the metabolic flux patterns
65 through the central C metabolic network as described in Dijkstra et al.¹ (Figure S2). It is
66 assumed in this model that glucose is the only C substrate utilized by microbes. All
67 model rates are expressed relative to glucose uptake (*v*_I), which is set at 100 moles. This

68 model has nine unknowns, seven of which are estimated using a known bacterial and
69 fungal metabolite precursor demand². In this paper, we assumed a fungi : bacteria ratio of
70 50:50 for the modeled microbial community. Previous studies have shown that
71 assumptions about microbial community composition do not much alter model MGE
72 estimates^{2,3}, because the average precursor requirements are not that different between
73 fungi and bacteria^{2,4}. The remaining two unknown model variables are then estimated
74 using the observed isotopologue ratios of glucose and pyruvate. The Excel linear
75 programming tool Solver was used to change the rates of $v14$ and $v10$ until modeled
76 isotopomer ratios matched observed values. The final output of the model is relative
77 rates for all 21 reactions of the central C metabolic network, which are used to calculate
78 MGE. The MGE is calculated from the uptake rate and CO₂ producing reactions ($v10$, $v5$,
79 $v7$ and $v8$) as:

$$80 \quad MGE = \frac{6*v1 - \Sigma CO_2}{6*v1} \quad (3)$$

81

82 ***III. Respiration and Microbial Biomass Measurements***

83 In a separate incubation two weeks after the final MGE measurement, we
84 assessed the effects of temperature on respiration and microbial biomass C (MBC)
85 concentration, and calculated the specific respiration rate ($\mu\text{g CO}_2\text{-C mg}^{-1} \text{MBC h}^{-1}$)(n=4).
86 In each incubator, we set up mason jars for each soil type following the same procedure
87 that we used for the metabolic tracer incubation. After a one-week incubation,
88 respiration rate was determined over 24 h using LICOR 6262 (LI-COR Biosciences,
89 Lincoln, NE). Afterwards, we determined MBC using the chloroform-fumigation
90 extraction method. Half of each sample was fumigated with chloroform for 7 days

91 (according to Haubensak et al.⁵) and extracted with 0.05 M K₂SO₄, while the other half
92 was immediately extracted with K₂SO₄. The extracted salt solution was oven-dried at
93 60 °C until dry, and analyzed for %C and %N on an elemental analyzer with IRMS. The
94 microbial biomass C and N were calculated as the difference between the fumigated and
95 immediately extracted samples, expressed as mg C or N g⁻¹ dry soil (Table S1). We
96 corrected microbial biomass C using an extraction efficiency (k_{EC}) of 0.45 for both soils⁶.
97 We used the extraction efficiency for nitrogen (k_{EN}) of 0.54 proposed by Brookes et al.⁷.
98

99 *IV. Calculation of Microbial Production and Turnover Rate.*

100 In our calculations, we assumed that 1) the MBC pool was at steady state, so
101 that net microbial growth was zero, and 2) all MBC that was turned over was turned
102 into CO₂. In section V, we will assess the sensitivity of our results to these
103 assumptions.

104 Total microbial respiration can be partitioned into

$$105 \quad R = R_g + R_\tau \quad (4),$$

106 with R_g and R_τ as, the amount of C respired while making microbial biomass and C
107 respired due to turnover (μg CO₂-C g⁻¹ soil d⁻¹) respectively.

108 New microbial biomass (ΔMBC_g; μg C g⁻¹ soil d⁻¹) is formed as follows,

$$109 \quad \Delta MBC_g = \frac{MGE}{1-MGE} * R_g \quad (5).$$

110 Under steady state conditions for the microbial biomass pool, an equal amount of
111 biomass is produced as is turned over and released as CO₂ (R_τ)

$$112 \quad \Delta MBC_g = \tau * MBC = R_\tau \quad (6).$$

113 Where τ, is the proportion of the microbial community that is turned over (d⁻¹).

114 Therefore respiration from turnover (R_τ) is equal to:

$$115 \quad R_\tau = \frac{MGE}{1-MGE} * R_g \quad (7).$$

116 Combining equation 4 and equation 1, total respiration (R) is equal to:

$$117 \quad R = R_g + \frac{MGE}{1-MGE} * R_g \quad (8).$$

118 So respiration from creating new microbial biomass (R_g) can be calculated as:

$$119 \quad R_g = \frac{R}{1 + \frac{MGE}{1-MGE}} = R(1 - MGE) \quad (9).$$

120 And respiration from turnover (R_τ) is:

$$121 \quad R_\tau = R - R_g = R(1 - (1 - MGE)) = R * MGE \quad (10).$$

122 And turnover (d^{-1}) is calculated as flux of C out of MBC divided by MBC:

$$123 \quad \tau = \frac{R_\tau}{MBC} = \frac{R * MGE}{MBC} \quad (11).$$

124 A conceptual diagram of these equations is available in Figure S3.

125

126 ***V. Sensitivity of Turnover to Calculation Assumptions***

127 *1) Non-Steady State MBC Pool*

128 When the MBC pool is not at steady state, ΔMBC_g is divided over turnover

129 and net microbial growth. So, ΔMBC_g is calculated as before (eq. 2). A portion of this

130 C is added to the MBC pool (ΔMBC_n),

$$131 \quad \Delta MBC_n = \alpha * \Delta MBC_g \quad (12)$$

132 while the remainder is lost as CO_2 due to turnover:

$$133 \quad \Delta MBC_g - \Delta MBC_n = (1 - \alpha)\Delta MBC_g = \tau * MBC \quad (13).$$

134 When $\alpha=1$, all MBC produced is added to the existing MBC, and no C is

135 available for turnover. When $\alpha=0$, then all MBC that is produced is turned over

136 (steady state assumption described above). When $\alpha < 0$, a net decline in MBC occurs,
 137 and more C is available for turnover than is produced.

138 Under these conditions, R_τ is calculated as

$$139 \quad \tau = \tau * MBC = (1 - \alpha)\Delta MBC_g \quad (14).$$

$$140 \quad R_\tau = (1 - \alpha) \left(\frac{MGE}{1 - MGE} \right) * R_g \quad (15).$$

$$141 \quad R = R_g + (1 - \alpha) \left(\frac{MGE}{1 - MGE} \right) * R_g \quad (16).$$

$$142 \quad R_g = \frac{R}{1 + (1 - \alpha) \left(\frac{MGE}{1 - MGE} \right)} = \frac{R(1 - MGE)}{1 - \alpha * MGE} \quad (17).$$

$$143 \quad R_\tau = R - R_g = R \left(1 - \frac{(1 - MGE)}{1 - \alpha * MGE} \right) \quad (18).$$

$$144 \quad \tau = \frac{R_\tau}{MBC + 0.5 * DMBC_n} = \frac{R}{MBC + 0.5 * DMBC_n} \left(1 - \frac{1 - MGE}{1 - \alpha * MGE} \right) \quad (19).$$

145 We assessed the sensitivity of our results to the assumption that MBC was at steady
 146 state, by calculating turnover rate assuming that there had been a 20 % increase in
 147 MBC over our incubation period. This is the same as testing $\alpha = 0.2$. There was no
 148 significant difference between microbial turnover rate calculated with the
 149 assumption of steady state MBC and microbial turnover rate calculated with an
 150 assumed 20 % increase in MBC (Figure S4).

151

152 2) Fate of C from Turnover

153 In the following equations, MBC that is turned over is respired (R_τ) or added
 154 to the SOC pool (ΔSOC)

$$155 \quad \tau * MBC = \Delta MBC_g = R_\tau + \Delta SOC \quad (20),$$

156 Introducing f as the fraction of microbial C that is being turned over into CO₂, and (1-
 157 f) as the fraction of microbial C that is turned over to dead SOC yields:

$$158 \quad R_{\tau} = f * \tau * MBC = f * \Delta MBC_g \quad (21).$$

$$159 \quad R_{\tau} = f \left(\frac{MGE}{1-MGE} \right) * R_g \quad (22).$$

$$160 \quad R = R_g + f \left(\frac{MGE}{1-MGE} \right) * R_g \quad (23).$$

$$161 \quad R_g = \frac{R}{1+f \left(\frac{MGE}{1-MGE} \right)} = \frac{R(1-MGE)}{1-(1-f)MGE} \quad (24).$$

$$162 \quad R_{\tau} = R - R_g = R \left(1 - \frac{(1-MGE)}{1-(1-f)MGE} \right) \quad (25).$$

163 and

$$164 \quad \tau = \frac{R_{\tau}}{f * MBC} = \frac{R}{f * MBC} \left(1 - \frac{(1-MGE)}{(1-(1-f)MGE)} \right) \quad (26).$$

165 We assessed the sensitivity of our results to the assumption that all turned over
 166 C is released as CO₂, by comparing calculated turnover rates under the “all C to CO₂”
 167 condition ($f=1$), with “all C to SOC pool” ($f=0$) and “C going for 50% to CO₂ and 50%
 168 to SOC” ($f=0.5$). When all or half the microbial turnover is directed to SOC, the
 169 calculated turnover rates are higher and the relationship with temperature is stronger
 170 (Figure S5). The assumption made in this experiment, that all turned over MBC goes
 171 to CO₂, represents the most conservative estimate of microbial turnover.

172

173 ***VI. Estimating Effects of Experiment Duration on MGE_A***

174 In most studies⁸⁻¹⁰, MGE is determined by adding a stable or radioactive isotope
 175 labeled substrate, followed by measuring the incorporation of the label into microbial
 176 biomass. Here MGE is calculated as:

177 $MGE = \frac{MBC}{S}$ (27)

178 or

179 $MGE = \frac{MBC}{MBC+R}$ (28)

180 where MBC is the labeled microbial C produced from the substrate-C added (S), and R as
 181 the labeled C respired as CO₂. As pointed out by Frey et al.¹¹, the two definitions of MGE
 182 are similar, unless a portion of S remains in the soil solution, or if some of the initial
 183 labeled MBC ends up as dead organic matter, but is not released as CO₂. We make the
 184 assumption that all S is taken up and turned into MBC at t=0 with an instantaneous MGE
 185 (MGE_I) = 0.72. At time 0, MBC equals:

186 $MBC_0 = MGE_I * S$ (29)

187 However, as soon as new microbial biomass is produced, it becomes susceptible to
 188 turnover (either viruses, grazing or natural senescence). So MBC₁ at t=1 becomes

189 $MBC_1 = MBC_0 - \tau * MBC_0 = (1 - \tau) * MBC_0$ (30)

190 with τ as the turnover rate (fraction of biomass that dies and is returned as CO₂ to the
 191 atmosphere and /or remains in the soil as dead organic matter). At t=2, MBC₂ becomes

192 $MBC_2 = (1 - \tau) * MBC_1 = (1 - \tau)^2 * MBC_0$ (31)

193 So, at t=n

194 $MBC_n = (1 - \tau)^n * MBC_0 = (1 - \tau)^n * MGE_I * S$ (32)

195 and

196 $MGE_A = \frac{((1-\tau)^n * MGE_I * S)}{S} = (1 - \tau)^n * MGE_I$ (33)

197

198 **VII. Statistical Analyses**

199 We performed a multifactor ANOVA on all experimental data using soil type and

200 incubation temperature as main factors. In two cases, the metabolic model could not find
201 matches with the observed isotopomer ratios. This was the case with one of the replicates
202 of mineral soil at 10 °C and mineral soil incubated at 15 °C, reducing the number of
203 replicates to 5 for modeled metabolic rates and MGE for these treatments. Microbial
204 biomass C and N data were log-transformed to meet the assumptions for ANOVA; the
205 microbial biomass N data had one outlier that was excluded from statistics. The
206 calculated microbial turnover and microbial production data were analyzed using a
207 regression analyses on the means from the bootstrap resampling against temperature.
208 Sensitivity analyses of assumptions used to calculate turnover were done using 95 % CI
209 of calculated turnover rates within each soil x temperature combination and using an
210 ANOVA on the regression of the mean turnover rates.

211

212 ***VIII. Microbial Enzyme Model***

213 We made two modifications to the Allison-Wallenstein-Bradford (AWB) microbial
214 model version in Li et al.¹². Instead of being constant, we made the microbial turnover
215 rate (τ_B) an Arrhenius function of temperature:

$$\tau_B(T) = \tau_{B,ref} * \exp \left[\frac{-Ea_\tau}{R} * \left(\frac{1}{T} - \frac{1}{T_{ref}} \right) \right] \quad (34)$$

216 where T is temperature (K), $\tau_{B,ref}$ is the microbial turnover rate at the reference
217 temperature T_{ref} (20°C or 293 K), R is the ideal gas constant (8.314 J mol⁻¹ K⁻¹) and Ea_τ is
218 the activation energy for microbial turnover (Table S3). The Arrhenius equation was used
219 as we expect sensitivity of microbial turnover to temperature to be driven by biological or
220 biochemical processes that do not usually respond linearly. The second modification was

221 to introduce a coefficient θ that determines the fraction of microbial turnover that enters
 222 soil carbon pools versus being respired to CO_2 . When $\theta = 1$, all dead microbial biomass
 223 enters soil carbon pools, and when $\theta = 0$, all dead biomass is respired to CO_2 . Although θ
 224 can vary, it was set to zero for all analyses reported here. The model equations are given
 225 below.

226 Microbial biomass (B) increases with DOC (D) uptake (F_U) times microbial
 227 growth efficiency (MGE) and declines with death (F_B) and enzyme production (F_E):

$$\frac{dB}{dt} = F_U * MGE - F_B - F_E \quad (35)$$

228 where assimilation is a Michaelis-Menten function scaled to the microbial biomass pool
 229 size:

$$F_U = \frac{V_U * B * D}{K_U + D} \quad (36)$$

230 and where E_C is a linear function of temperature with intercept MGE_{ref} and slope m :

$$E_C(T) = MGE_{ref} + m * (T - T_{ref}) \quad (37)$$

231 Microbial biomass turnover is modeled as a first-order process with the temperature-
 232 sensitive rate constant τ_B :

$$F_B = \tau_B * B \quad (38)$$

233 Enzyme production is modeled as a constant fraction (τ_E) of microbial biomass:

$$F_E = \tau_E * B \quad (39)$$

234 Temperature sensitivities for V , V_U , K , and K_U follow the Arrhenius relationship as in Eq.
 235 34. CO_2 respiration is the fraction of DOC that is not assimilated into MBC plus the
 236 respired fraction of microbial biomass turnover:

$$C_R = F_U * (1 - MGE) + F_B * (1 - \theta) \quad (40)$$

237 The enzyme pool (E) increases with enzyme production and decreases with enzyme
 238 turnover:

$$\frac{dE}{dt} = F_E - F_L \quad (41)$$

239 where enzyme turnover is modeled as a first-order process with a rate constant τ_L :

$$F_L = \tau_L * E \quad (42)$$

240 The SOC pool (S) increases with external inputs and a fraction of dead microbial biomass
 241 ($a_{BS} * \theta$) and decreases due to decomposition losses:

$$\frac{dS}{dt} = I_S + F_B * a_{BS} * \theta - F_S \quad (43)$$

242 where decomposition of SOC is catalyzed according to Michaelis-Menten kinetics by the
 243 enzyme pool:

$$F_S = \frac{V * E * S}{K + S} \quad (44)$$

244 The DOC pool receives external inputs, a fraction of dead microbial biomass, the
 245 decomposition flux, and dead enzymes, while assimilation of DOC by microbial biomass
 246 is subtracted:

$$\frac{dD}{dt} = I_D + F_B * (1 - a_{BS}) * \theta + F_S + F_L - F_U \quad (45)$$

247 The steady-state analytical solutions for SOC, DOC, MBC, and ENZC are given here:

$$S = \frac{-K * \tau_L * (x_1 * \tau_E + x_2 * MGE * \tau_B * \theta - I_S * \tau_B)}{\tau_E * ((I_S + I_D) * MGE * V + x_1 * \tau_L) + \tau_L * \tau_B * (x_2 * MGE * \theta - I_S)} \quad (46)$$

248 where

$$x_1 = I_S * (MGE - 1) \text{ and } x_2 = I_S - a_{BS} * (I_D + I_S) \quad (47)$$

$$D = \frac{-K_U * (\tau_B + \tau_E)}{\tau_B + \tau_E - MGE * V_U} \quad (48)$$

$$B = \frac{MGE * (I_D + I_S)}{(1 - MGE) * \tau_E + \tau_B * (1 - MGE * \theta)} \quad (49)$$

$$E = \frac{B * \tau_E}{\tau_L} \quad (50)$$

249 To generate Figure 4, we calculated the relative change in steady-state solutions for SOC
 250 and MBC at from 0 to 20°C under three scenarios with $\theta = 0$, meaning that all microbial
 251 turnover is respired as CO₂. For the “constant turnover, constant MGE” scenario, $Ea_i = 0$
 252 kJ mol⁻¹ and $m = 0$. For the “constant microbial turnover, declining MGE” scenario, $Ea_i =$

253 0 kJ mol^{-1} and $m = -0.016 \text{ }^{\circ}\text{C}^{-1}$. For the “increasing microbial turnover, constant MGE”

254 $E_a = 47 \text{ kJ mol}^{-1}$ and $m = 0$.

255 **SUPPLEMENTARY NOTE**

256 *Thermodynamic Limits to MGE.*

257 The value of MGE in soil microbial communities is important for our
258 understanding of soil C cycling processes. This value is explicitly or implicitly part of
259 soil C cycling models, usually a constant value is used^{8,13,14} ranging from 0.15 to 0.60
260 (ref. 13).

261 Efforts to predict MGE from thermodynamic and chemical principles have
262 been ongoing for several decades^{15,16}. Experimental data are mostly limited to pure
263 culture studies where substrate availability is usually high relative to substrate
264 availabilities in natural environments. MGE is limited by thermodynamic constraints¹⁴.
265 The theoretical maximum value of MGE was calculated in several studies. The
266 thermodynamic maximum yield can be predicted from the ratio between the degree of
267 reduction of the substrate (e.g., glucose $\gamma_s = 4$ or formate $\gamma_s=2$) and product, (γ_p biomass \sim
268 4.2)¹⁷. The MGE_{max} is about 0.95 (ref. 13, 16). A second theoretical maximum is defined
269 by the cost of making new biomass. This yields an MGE_{max} from glucose of about 0.88
270 (ref. 4). The observed MGE values in this study (MGE ranged from 0.67 to 0.75) were
271 lower than the MGE_{max} values identified above, but higher than the average
272 thermodynamic efficiency in pure culture studies^{13,14,16}.

273 Variability of yield (MGE) in culture studies spans almost two orders of
274 magnitude from 0.01 to 0.8 (ref. 15-19) associated with species differences, substrate
275 type and concentration, and environmental factors. Experimental values for MGE in pure
276 culture studies are always lower than the theoretical maximal yield values described
277 above. The ratio between experimentally observed MGE_{max} and the theoretical MGE_{max}

278 is called the thermodynamic efficiency¹³⁻¹⁶. This value is used as a “first approximation”
279 according to Roels 1980¹⁶, and should not be mistaken for a theoretical thermodynamic
280 maximal yield, as higher values have been observed in pure culture studies^{15,16,18,19} and
281 soil and aquatic ecosystems (ranging from close to zero to >0.8 for both environments¹³).

282 **SUPPLEMENTARY TABLES**

283

284 **Table S1.** Microbial biomass C (MBC) and microbial biomass N (MBN) means and
 285 standard error for four incubation temperatures and two soil types (n=4). Microbial
 286 biomass was calculated using $k_{EC} = 0.45$ and $k_{EN} = 0.54$.

Temperature (°C)	MBC ($\mu\text{g g}^{-1}$ dry soil)		MBN ($\mu\text{g g}^{-1}$ dry soil)	
	Mineral Soil	Organic Soil	Mineral Soil	Organic Soil
5	276 ± 33	1,229 ± 117	37.7 ± 2.4	120 ± 9.4
10	236 ± 8.8	1,585 ± 200	35.8 ± 0.7	165 ± 32
15	282 ± 43	1,623 ± 170	36.9 ± 3.2	182 ± 16
20	263 ± 9.3	1,412 ± 81	35.0 ± 3.0	139 ± 7.7

287

288

289 **Table S2.** Glucose and pyruvate isotopomer ratios for mineral and organic soil at 5, 10,
 290 15, and 20 °C (means ± standard error, n=6 except organic soil at 5 °C; n=5).

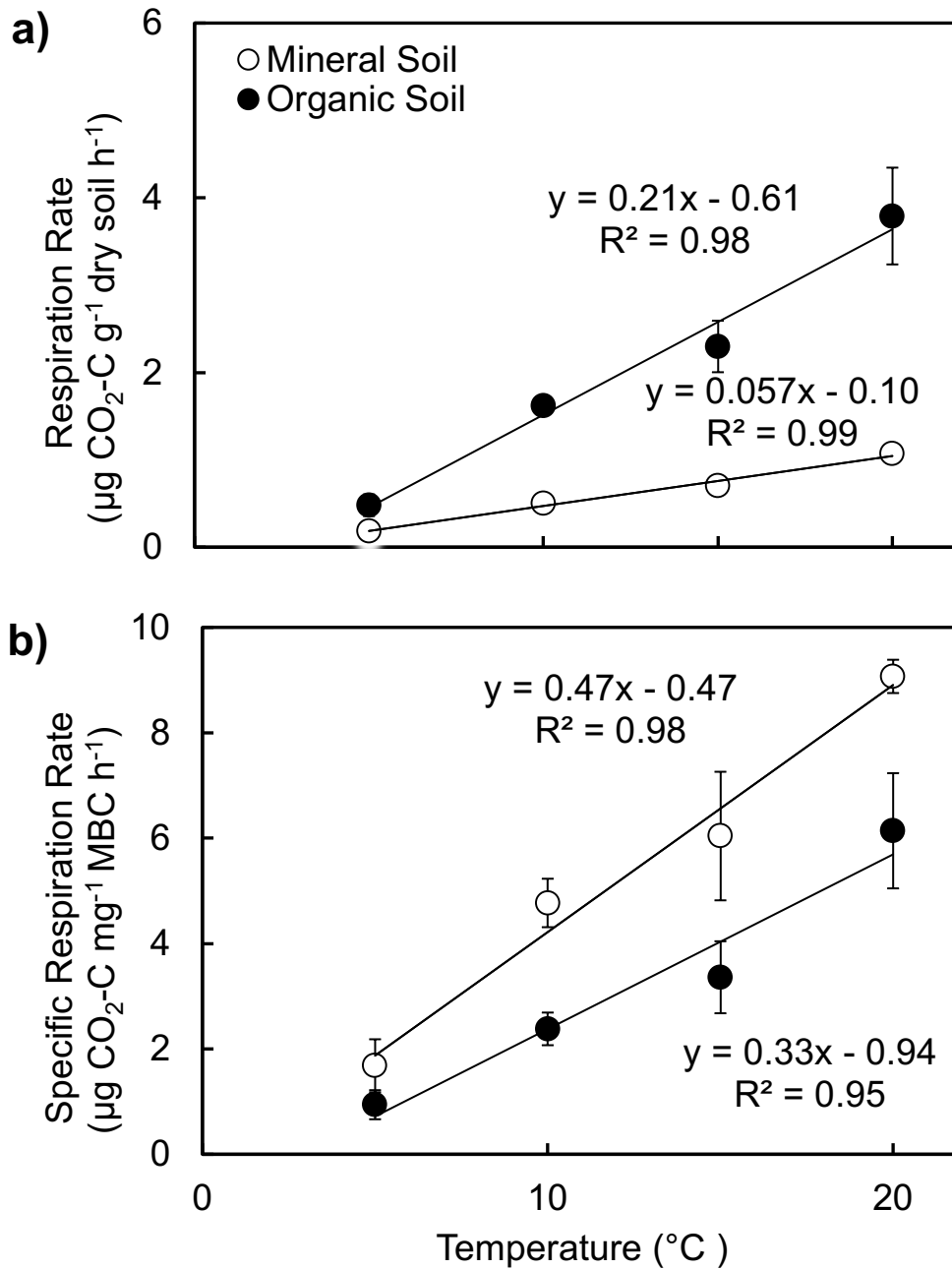
Temperature (°C)	C ₀ /C ₁ Ratio of Glucose		C ₁ /C ₂₃ Ratio of Pyruvate	
	Mineral Soil	Organic Soil	Mineral Soil	Organic Soil
5	3.21 ± 0.31	2.92 ± 0.24	4.41 ± 0.40	3.56 ± 0.20
10	3.26 ± 0.15	2.91 ± 0.14	3.38 ± 0.20	3.73 ± 0.35
15	3.60 ± 0.39	2.94 ± 0.16	3.75 ± 0.30	3.51 ± 0.19
20	2.70 ± 0.12	3.15 ± 0.26	3.94 ± 0.46	3.61 ± 0.31

291

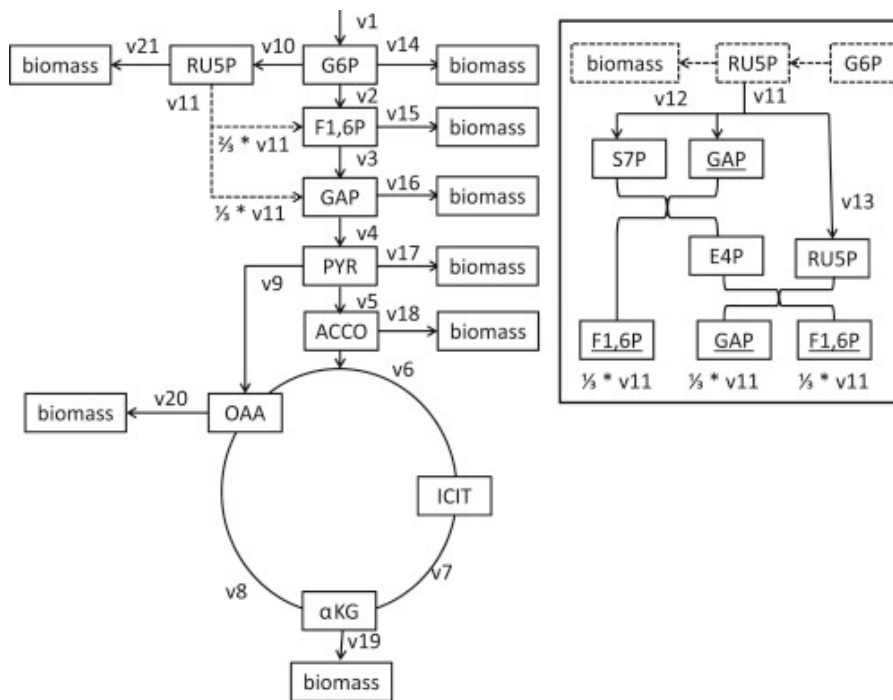
292 **Table S3.** Microbial- enzyme model parameter descriptions, values, and units.

Parameter	Description	Value	Units
T_{ref}	Reference temperature	20	°C
MGE_{ref}	MGE at reference temperature	0.31	
m	MGE change with temperature	[0, -0.016]	°C ⁻¹
I_S	SOC input rate	0.00015	mg C g ⁻¹ soil h ⁻¹
I_D	DOC input rate	0.00001	mg C g ⁻¹ soil h ⁻¹
V_{ref}	SOC reference V_{max}	1	mg C mg ⁻¹ C h ⁻¹
$V_{U,ref}$	DOC uptake reference V_{max}	0.01	mg C mg ⁻¹ MBC h ⁻¹
K_{ref}	SOC reference K_m	250	mg C g ⁻¹ soil
$K_{U,ref}$	DOC uptake reference K_m	0.26	mg C g ⁻¹ soil
$\tau_{B,ref}$	Reference MBC turnover rate	0.00028	mg C mg ⁻¹ C h ⁻¹
Ea_V	SOC V_{max} activation energy	47	kJ mol ⁻¹ K ⁻¹
Ea_{VU}	Uptake V_{max} activation energy	47	kJ mol ⁻¹ K ⁻¹
Ea_K	SOC K_m activation energy	30	kJ mol ⁻¹ K ⁻¹
Ea_{KU}	Uptake K_m activation energy	30	kJ mol ⁻¹ K ⁻¹
Ea_τ	MBC turnover activation energy	47	kJ mol ⁻¹ K ⁻¹
τ_E	Enzyme production rate	5.6×10^{-6}	mg C mg ⁻¹ MBC h ⁻¹
τ_L	Enzyme loss rate	0.001	mg C mg ⁻¹ C h ⁻¹
a_{BS}	Fraction of dead MBC partitioned to SOC	0.5	
θ	Fraction of dead MBC transferred to soil pools	0	

293



297 **Figure S1.** Response of a) soil respiration rate and b) specific respiration rate of mineral
 298 and organic soil to temperature (means and se; some standard errors are smaller than data
 299 points).

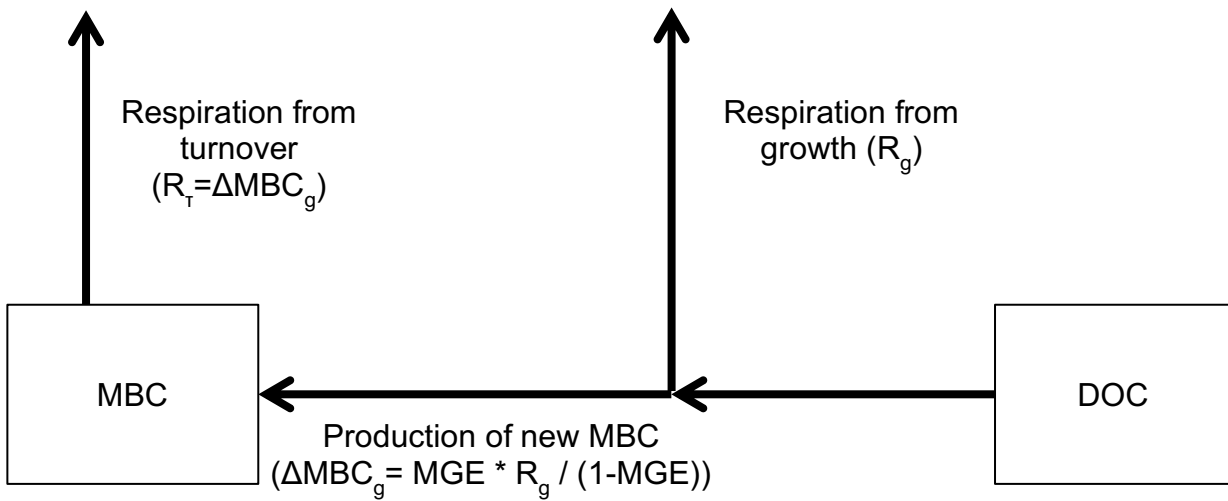


300

301 **Figure S2.** Model for metabolic processes in soil microbial communities. Flux rates (v2-
 302 v21) are normalized relative to glucose uptake (v1, set at 100 moles). Insert depicts
 303 details of the pentose phosphate pathway. Abbreviations: G6P, glucose-6-phosphate;
 304 F1,6P, fructose-1,6-phosphate; GAP, glyceraldehyde-phosphate; PYR, pyruvate; ACCO,
 305 acetyl-CoA; ICIT, isocitrate; α KG, α -ketoglutarate; OAA, oxaloacetate; RU5P, ribulose-
 306 5-phosphate; S7P, sedoheptulose-7-phosphate; E4P, erythrose-4-phosphate. Reprinted
 307 from ref. 1.

308

309



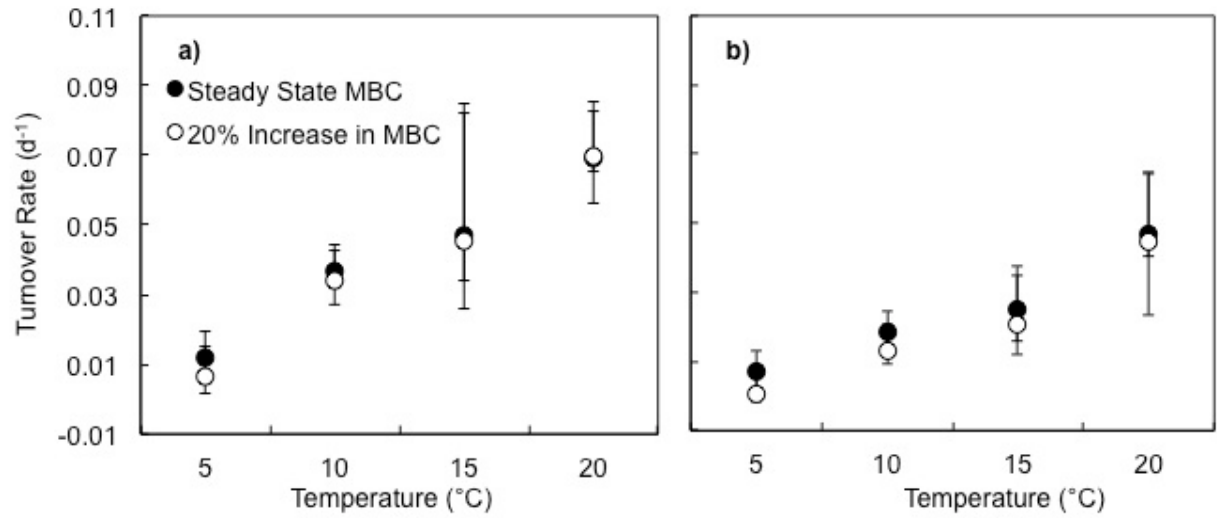
310

311 **Figure S3.** Schematic showing relationships between measured (total respiration, MGE,

312 and MBC pool) and calculated values (production rate and turnover rate). Total

313 respiration rate is the sum of respiration from turnover and growth ($R = R_g + R_T$).

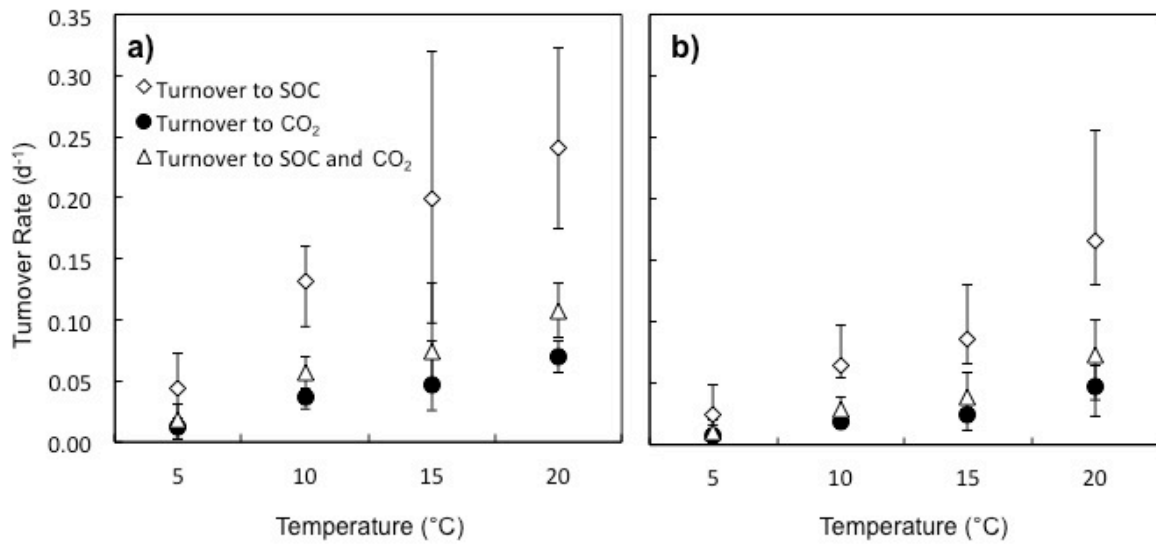
314



315

316 **Figure S4.** Effect of change in MBC on calculated microbial turnover rates at each
 317 temperature for a) mineral soil and b) organic soil (means and 95% CI).

318



319

320 **Figure S5.** Effect of changing the fate of turned over MBC on calculated microbial

321 turnover rates for a) mineral soil and b) organic soil (means and 95% CI).

322 **SUPPLEMENTARY REFERENCES**

323

324 1. Dijkstra, P. *et al.* Effect of temperature on metabolic activity of intact microbial
325 communities: Evidence for altered metabolic pathway activity but not for
326 increased maintenance respiration and reduced carbon use efficiency. *Soil*
327 *Biology & Biochemistry* **43**, 2023-2031, doi:10.1016/j.soilbio.2011.05.018
328 (2011).

329 2. Dijkstra, P. *et al.* Modeling soil metabolic processes using isotopologue pairs of
330 position-specific C-13-labeled glucose and pyruvate. *Soil Biology &*
331 *Biochemistry* **43**, 1848-1857, doi:10.1016/j.soilbio.2011.05.001 (2011).

332 3. van Groenigen, K. J. *et al.* Using metabolic tracer techniques to assess the impact of
333 tillage and straw management on microbial carbon use efficiency in soil. *Soil*
334 *Biology & Biochemistry* **66**, 139-145, doi:10.1016/j.soilbio.2013.07.002
335 (2013).

336 4. Gommers, P. J. F., Vanschie, B. J., Vandijken, J. P. & Kuenen, J. G. Biochemical limits
337 to microbial-growth yields - an analysis of mixed substrate utilization.
338 *Biotechnology and Bioengineering* **32**, 86-94, doi:10.1002/bit.260320112
339 (1988).

340 5. Haubensak, K. A., Hart, S. C. & Stark, J. M. Influences of chloroform exposure time
341 and soil water content on C and N release in forest soils. *Soil Biology &*
342 *Biochemistry* **34**, 1549-1562, doi:10.1016/s0038-0717(02)00124-4 (2002).

343 6. Wu, J., Joergensen, R. G., Pommerening, B., Chaussod, R. & Brookes, P. C.

344 Measurement of soil microbial biomass c by fumigation extraction - an

- 345 automated procedure. *Soil Biology & Biochemistry* **22**, 1167-1169,
346 doi:10.1016/0038-0717(90)90046-3 (1990).
- 347 7. Brookes, P. C., Landman, A., Pruden, G. & Jenkinson, D. S. Chloroform fumigation
348 and the release of soil-nitrogen - a rapid direct extraction method to measure
349 microbial biomass nitrogen in soil. *Soil Biology & Biochemistry* **17**, 837-842,
350 doi:10.1016/0038-0717(85)90144-0 (1985).
- 351 8. Frey, S. D., Lee, J., Melillo, J. M. & Six, J. The temperature response of soil microbial
352 efficiency and its feedback to climate. *Nature Climate Change* **3**, 395-398,
353 doi:10.1038/nclimate1796 (2013).
- 354 9. Steinweg, J. M., Plante, A. F., Conant, R. T., Paul, E. A. & Tanaka, D. L. Patterns of
355 substrate utilization during long-term incubations at different temperatures.
356 *Soil Biology & Biochemistry* **40**, 2722-2728,
357 doi:10.1016/j.soilbio.2008.07.002 (2008).
- 358 10. Tucker, C. L., Bell, J., Pendall, E. & Ogle, K. Does declining carbon-use efficiency
359 explain thermal acclimation of soil respiration with warming? *Global Change*
360 *Biology* **19**, 252-263, doi:10.1111/gcb.12036 (2013).
- 361 11. Frey, S. D., Gupta, V., Elliott, E. T. & Paustian, K. Protozoan grazing affects
362 estimates of carbon utilization efficiency of the soil microbial community. *Soil*
363 *Biology & Biochemistry* **33**, 1759-1768, doi:10.1016/s0038-0717(01)00101-
364 8 (2001).
- 365 12. Li, J. W., Wang, G. S., Allison, S. D., Mayes, M. A. & Luo, Y. Q. Soil carbon sensitivity
366 to temperature and carbon use efficiency compared across microbial-

- 367 ecosystem models of varying complexity. *Biogeochemistry* **119**, 67-84,
368 doi:10.1007/s10533-013-9948-8 (2014).
- 369 13. Manzoni, S., Taylor, P., Richter, A., Porporato, A. & Agren, G. I. Environmental and
370 stoichiometric controls on microbial carbon-use efficiency in soils. *New*
371 *Phytologist* **196**, 79-91, doi:10.1111/j.1469-8137.2012.04225.x (2012).
- 372 14. Sinsabaugh, R. L., Manzoni, S., Moorhead, D. L. & Richter, A. Carbon use efficiency
373 of microbial communities: stoichiometry, methodology and modelling.
374 *Ecology Letters* **16**, 930-939, doi:10.1111/ele.12113 (2013).
- 375 15. Heijnen, J. J. in *Biosystems Engineering Ii: Linking Cellular Networks and*
376 *Bioprocesses* Vol. 121 *Advances in Biochemical Engineering-Biotechnology*
377 (eds C. Wittmann & R. Krull) 139-162 (2010).
- 378 16. Roels, J. A. Application of macroscopic principles to microbial-metabolism.
379 *Biotechnology and Bioengineering* **22**, 2457-2514,
380 doi:10.1002/bit.260221202 (1980).
- 381 17. Xiao, J. H. & VanBriesen, J. M. Expanded thermodynamic model for microbial true
382 yield prediction. *Biotechnology and Bioengineering* **93**, 110-121,
383 doi:10.1002/bit.20700 (2006).
- 384 18. von Stockar, U., Vojinovic, V., Maskow, T. & Liu, J. Can microbial growth yield be
385 estimated using simple thermodynamic analogies to technical processes?
386 *Chemical Engineering and Processing* **47**, 980-990,
387 doi:10.1016/j.cep.2007.02.016 (2008).
- 388 19. Heijnen, J. J. & Vandijken, J. P. In search of a thermodynamic description of
389 biomass yields for the chemotropic growth of microorganisms - response.

390 *Biotechnology and Bioengineering* **42**, 1127-1130,

391 doi:10.1002/bit.260420916 (1993).

392